STUDY OF HEAT AND FLUID FLOW IN DOUBLET ENHANCED GEOTHERMAL SYSTEMS

by

Pranay Ashok Asai

A thesis submitted to the faculty of
The University of Utah
in partial fulfillment of the requirements for the degree of

Master of Science

in

Petroleum Engineering

Department of Chemical Engineering

The University of Utah

December 2017

Copyright © Pranay Ashok Asai 2017

All Rights Reserved

The University of Utah Graduate School

STATEMENT OF THESIS APPROVAL

The thesis of **Pranay Ashok Asai**

has been approved by the following supervisory committee members:

John McLennan	, Chair	**10/18/2017** Date Approved
Milind Deo	, Member	**10/18/2017** Date Approved
Joseph Moore	, Member	**10/18/2017** Date Approved

and by **Milind Deo** , Chair/Dean of

the Department/College/School of **Chemical Engineering**

and by David B. Kieda, Dean of The Graduate School.

ABSTRACT

Geothermal energy is the future for producing clean and renewable energy. The energy from geothermal reservoirs can be recovered using Enhanced Geothermal Systems (EGS). EGS consists of two or more wells drilled into the thermal reservoir and connected by planar hydraulic fractures. A working fluid is then circulated inside the system to extract the heat to the surface. To design an efficient system, it is important to understand how performance of the EGS is affected by different parameters. This can be done by carrying out different simulations for the EGS.

Simulating a geothermal reservoir is complex and time consuming, mainly because of its nonisothermal nature and enormous size. In this study, various issues related to simulation of Enhanced Geothermal System (EGS) are investigated and practical solutions are proposed. A comprehensive study was conducted to show the effect of grid size on predictions of temperature of the produced water. Simulations were carried out to study the effect of five parameters (wellbore inclination, well spacing, fracture spacing, injection rate, and injection temperature) on the total heat production from a doublet multifractured system, over a period of 30 years. The CMG STARS simulator was used to model a 30-year-long production schedule. This simulator incorporates heat and mass flow through the porous media although there is no thermoelastic coupling. Another study emphasizes the distribution of flow among the fractures in a multifractured doublet system. An analytical model (analogous to Kirchhoff's law) was developed to distribute the flow in the system.

All these studies would be useful in systematic evaluation of EGS and provide guidance to design and develop optimal EGS.

Dedicated To my father *Ashok Asai*, mother *Lalita Asai*
My loving brother *Pratik Asai*
My Sweetheart *Sreejita Saha*

For their love, support, and encouragement

Thank you all for believing in me

TABLE OF CONTENTS

LIST OF TABLES

Tables

LIST OF FIGURES

Figures

ACKNOWLEDGMENTS

First and foremost, I would like to thank my research advisor Dr. John McLennan for giving me an opportunity to work on this research. I would also like to thank him for his endless support and all the help that he has given me that aided in my completion of this research. I am thankful to Dr. Joseph Moore for his guidance on enhanced geothermal systems. I am thankful to Dr. Palash Panja for helping me with CMG STARS simulations and writing technical papers. I would like to thank my committee member Dr. Milind Deo for agreeing to serve on my committee and helping me throughout the process. I thank Sreejita Saha and Anuj Kapoor for their help in reviewing the contents for my thesis. I would like to thank everyone at FORGE Utah for the data they have provided for my research. I would also like to thank EGI for providing me resources required for my research. I would like to thank all my batch mates and friends at EGI. Finally, I would like to thank my parents, Ashok and Lalita Asai, and my brother, Pratik, for their love and support throughout my entire life. Without them, I would not be where I am today.

Thanks to everyone,

Pranay Asai

CHAPTER 1

INTRODUCTION

1.1 What Is Geothermal Energy?

Geothermal energy is a naturally occurring source of heat energy present in the subsurface of the Earth's crust. It is clean and sustainable over a long period. The geothermal reservoirs range from shallow depth hot rock to deeper and extremely high temperatures of molten rock called magma. This heat can be recovered by circulating water or any other fluid to carry the heat to the surface. The heat from the geothermal reservoir can be directly used for household heating systems or to produce electricity, depending on the temperature for the produced fluid.

1.2 What Is Enhanced Geothermal System (EGS)?

Not all the geothermal reservoirs have a fractured hot dry rock that can be used readily to circulate the working fluid to extract heat. This makes the availability of natural fractures a necessity to extract the heat. A proposed solution to overcome this problem involves drilling of two or more wells and creating hydraulic fractures to interconnect the wells, creating a closed loop system to circulate the fluid. This is known as an Enhanced Geothermal System.

1.3 Study of EGS

1.3.1 Simulation of EGS

Development of EGS is a huge capital investment, making it necessary to design an efficient system. This can be done by simulating the EGS and studying its performance under different conditions. Because of its large size, there are some challenges that are faced in simulation of an EGS. Chapter 2 addresses these challenges and provides solutions to overcome them.

1.3.2 Parameters Affecting EGS Performance

There are many factors that affect the performance of an EGS. Chapter 3 talks about the effect of five different parameters (well spacing, fracture spacing, wellbore inclination, injection temperature, and injection flow rate) on the total heat recovery in multifractured doublet systems, over a period of 30 years. The factors are ranked depending on the extent they impact the heat production in a given time period. This provides guidelines and a step-wise approach towards development of an efficient system.

1.3.3 Flow Distribution in EGS

For efficient design of EGS with maximum heat recovery factor, it is important to study the flow distribution in the system. Chapter 4 emphasizes the need of flow distribution in multifractured doublet systems and a generalized equation for flow distribution in individual fractures is given. It also evaluates the different factors that guides this flow distribution among the fractures.

CHAPTER 2

SIMULATING AN ENHANCED GEOTHERMAL SYSTEM (EGS) WITH INCLINED WELLS AND HYDRAULIC FRACTURES: ISSUES AND UPSCALING[1]

2.1 Abstract

An increasing demand for clean energy with minimum environmental impact justifies development of geothermal energy. Simulating a geothermal reservoir is complex and time consuming, mainly because of its nonisothermal nature and enormous size. In this study, various issues related to simulation of enhanced geothermal system (EGS) are investigated and practical solutions are proposed. A comprehensive study was conducted to show the effect of grid size on predictions of temperature of the produced water. It is also shown that the performance of EGS is affected by the fracture conductivity rather than the individual values of permeability and width. A simplified model is proposed in this study to reduce the run time significantly (1.5 to 14 times) without sacrificing accuracy in the results. In the proposed model, only two simulations of small parts of top and bottom portions of the reservoir with two fractures are run to represent the entire reservoir. The proposed model is tested in different scenarios created by varying the well inclination angle, fracture spacing, and well spacing. Value of R^2 close to unity (0.96 to 1.0) and

1 Pranay Asai, University of Utah; Palash Panja, University of Utah; John McLennan, University of Utah; Joseph Moore, University of Utah

smaller value of AARE (less than 3%) indicate the acceptance of the proposed model.

2.2 Keywords

Simulation issues; Enhanced Geothermal System (EGS); up-scaling; simplified model; grid sensitivity; fracture conductivity

2.3 Introduction

The HDR (Hot Dry Rock) is a very old concept [1-3] which, with the help of EGS (Enhanced Geothermal System) [4, 5], can be a potential energy source. It works on the principle of extracting the heat from the subsurface by using a fluid medium to transport the heat to the surface. EGS used in a closed loop system is an efficient system as this helps to minimize the water losses and prolong the life of the EGS system by only extracting the desired amount of heat. The potential of a geothermal reservoir is determined by the formation type, continuity of the formation, heat capacity, heat conductivity, and the geothermal gradient. A geothermal system having a thermal gradient greater than 55°C/km at a depth of 2km to 3km with a reference temperature of 200°C is considered to be an economically viable investment in terms of energy recovery.

Planning and creating an EGS is a huge capital investment and hence, development of an efficient system is needed [6]. The simulation of an EGS plays an important role in planning and development of the system by giving a better understanding regarding the heat extraction, depletion, and longevity of the EGS. The data obtained from the geothermal site can be used to create a numerical model and the simulations can be manipulated numerous times to design the best possible and the most efficient way to

extract the heat from the reservoir. This helps in minimizing the risk and optimizing the heat extraction capabilities within the available constraints.

Many extensive studies have been carried out in the realm of geothermal heat extraction for different conceptual designs like a doublet (with a production and an injection well) or a triplet (two production wells and an injection well), either drilled vertically or horizontally, but there are rarely any studies on angular wells. However, none of them specifically mentions the challenges that are faced during the modeling of the EGS system. When the EGS is drilled horizontally, the scaling-up is not an issue as all the fractures (if equally spaced) can be considered identical and can be scaled up linearly. But when the wells are vertical or inclined, scaling-up using a single fracture or a single group of fractures would not yield correct results because the temperature keeps changing with depth. Yidong Xia et al. [7] studied the effect of fracture spacing for horizontal and inclined wells for the doublet system by simulation of a group of five fractures along the well and then scaling it up, without mentioning how they scaled it up for the angular wells. Yu-Chao Zeng et al. [8] studied the heat extractions with 2D fracture modeling and concluded that the EGS is sensitive towards flow rate and injection temperature. Wenbo Huang et al. [9] studied the EGS performance and concluded that heterogeneity plays an important role and the temperature decline is affected by the seepage flow in the reservoir. Though all these studies and hypothetical model development have helped in developing a better understanding of the heat extraction, none of them specifically mentions the challenges faced in modeling and simulation of the EGS.

The objective of this study is to address the hurdles encountered while modeling the thermal reservoir and how to overcome them. We simulated the EGS using the

commercial reservoir modeling software, CMG. The need for the proper gridding [10] of the reservoir is discussed to incorporate the small changes as well as save time due to excessive gridding. This study also focuses on choosing optimum fracture size without affecting the fracture conductivity to help in proper reservoir modeling. We will also talk about designing a better model for the reservoir that would tremendously reduce the simulation time, without actually having to simulate the entire model and yet producing accurate results. The new model is flexible enough to incorporate changes in well spacing, fracture spacing, and the angle of the well. This model will help in saving overall time in design of the simulation, as well as running the simulation. This also means that it could be carried out without the need of high computational capacities, making it portable and cost efficient.

2.4 Simulation of Enhanced Geothermal System

There are many well configurations (doublet, triplet etc.) for optimized heat recovery from EGS. In this study, a doublet system is selected to accomplish the objectives. A schematic diagram of a doublet system with one vertical fracture connecting the production well and injection well is shown in Figure 2.1.

The well inclination is measured from the vertical axis as shown in Figure 2.1. Well spacing is measured as the perpendicular distance between the two wells, whereas fracture spacing is the horizontal spacing between two consecutive fractures. Typically, the injection well is placed below the production well so that the injected water flows upward from the higher temperature region towards the lower one. Injected water is distributed among the vertical fractures according to different pressures in the fractures, whereas the

heat flows dominantly in the horizontal direction by convection from formation to injected water in a vertical fracture.

Parameters used in this study resemble the data from Frontier Observatory for Research in Geothermal Energy (FORGE program by the U.S. Department of Energy) site at Milford, Utah. The temperature gradient is 60 ^{O}C/km with the reference temperature of 200 ^{O}C at 2500 meters depth. The site has a granite formation that has low porosity of 1% and low permeability around 200μD to 1000μD. The wells in EGS are generally very long with several hydraulic fractures to increase the surface area of interaction within the reservoir. For example, in a doublet system, 1200m long wells are expected with inclination of 60 degrees (injection well kick off at the depth of 1460m, and toe of the well at 2520m). For 100m fracture spacing, approximately 11 hydraulic fractures (the horizontal distance between toe and heel of the well is around 1040m) are required and each fracture connects injection and production wells for circulation of injected water.

This study focuses on the need for development of efficient simulations for the EGS that would be less time consuming and just as accurate as current methods. A commercial simulator, STARS, from Computer Modeling Group, Calgary, Canada (CMG) is used here for reservoir simulation with heat and mass transfers. To avoid the complexity of hydraulic fracture, simple planar fractures were simulated that consist of grids with higher permeability and porosity than the surrounding reservoir. These grids can emulate a fracture effectively to carry out the studies. All the simulated factures were assumed to be uniform and isotropic in nature having the same fracture conductivity.

2.5 Sensitivity to Grid Size

The model created in the CMG requires the reservoir to be distributed into small grid blocks. Each individual grid block is isotropic in nature for which the properties and the initial conditions are defined individually at the start of the simulation. Therefore, fewer grid blocks (which means larger grid blocks for the same reservoir size) do not represent the reservoir accurately, especially when there is a temperature gradient in the reservoir and thus, results may be less accurate with irregularities and discrepancies. However, reducing the grid block size, which increases the number of grid blocks, is a better representation of the actual reservoir. On the other hand, it takes a longer time to initialize, run, and process. This calls for an optimization study to choose grid size that is able to accurately predict the results in less time. In this section, effect of grid size on results in terms of produced water temperature is investigated.

Different grid sizes in all the directions are defined individually according to the Cartesian coordinate system. Grids along the z-axis are refined in the EGS model in order to represent temperature in the reservoir more accurately due to a geothermal gradient. The grids along the y-axis need refinement as well because of the fluid movement in the y-z plane, where the convective and conductive heat transfers take place between the reservoir and the fluid. The fluid flow along the x-axis is almost negligible and the heat transfer in the reservoir is dominantly due to conduction, which depends only on the temperature gradient, hence the grids along the x-axis can be a bit coarser than those along y-axis or z-axis. For example, a diagram showing the progressive refinement of grid size from coarse to fine along the x-z plane is shown in Figure 2.2.

To understand the effect of grid size in a better way, five different grid sizes for

each x, y, and z direction are chosen in this study. Thirteen simulations (few simulations are common) were carried out with a base case (Simulation 3) consisting of 58, 77, and 367 grid blocks in the x, y, and z direction, respectively, as shown in Table 2.1. The base case was chosen in such a way that it gave proper results with minimum or acceptable errors and would also require less run time.

Simulations 1 through 5 were intended to study the effect of refinement in the x-direction where number of grid blocks in the x-direction is varied keeping the same numbers of grid blocks in the y and z direction. Similarly, simulations 6 through 9 and 10 through 13 were designed to study the effects of refinement along the y and z directions by keeping the same number of grid blocks in the other two directions.

The effect of different grid sizes is dominant near the major dynamic locations such as near the fracture zone and the wellbores, because of a huge difference in the properties of the grids (mainly porosity, permeability, and temperature). Therefore, instead of having a uniform division of grid blocks, it is beneficial to have varying grid block sizes, which are finer near the dynamic zones but get coarser away from them (see Figure 2.3). This helps in reducing the total number of grid blocks and hence reducing the computational time.

After running all simulations, the improvements in results due to finer grids is measured by the error calculations in terms of average absolute relative error (AARE, see Appendix A) with respect to the base case (Simulation 3) as shown in Table 2.2. It was observed that the temperature decline curve for the produced water over 30 years was not affected much by variation in the number of grid blocks along the x-axis (see Figure 2.4). Though the coarseness is observed visually with larger grid sizes (see Figure 2.5), there is

no major effect on the temperature decline curve, as long as some portion near the fracture is composed of refined grids (up to 7m on both sides of the fracture to incorporate the near fracture zone). This gives us the liberty of choosing larger grid blocks along the x-axis, reducing the overall grids and thus the simulation time, whereas along the y-axis (see Figure 2.6) and z-axis (see Figure 2.7), the peak of the temperature decline curve changes and hence is required to be refined to a point when no further changes are observed in the decline curve. It is also evident for Figure 2.8 and Figure 2.9 that the coarseness in the grid size does not distribute the temperature properly along the cross-section of the reservoir, which leads to improper calculation for temperature over time. Figure 2.5, Figure 2.8, and Figure 2.9 show the temperature gradient cross-section of the reservoir after 20 years; as the number of grid blocks increases, the temperature gradient becomes more accurate and smooth in nature, leading to better accuracy. However, as more grid blocks would take longer time to be processed, a base case (58, 77, 367) was chosen to carry out all the further studies as it gave results with minimum errors and in less time.

2.6 Representing Vertical Fractures

The fluid flow rate in the fracture is governed by the fracture conductivity, which is the product of the fracture width and the fracture permeability. As long as the fracture conductivity remains constant, the same results are obtained from the simulations, meaning a 0.001m wide fracture with a permeability of 500000mD (fracture conductivity of 500mD.m) provides similar results with fracture width of 0.01m and fracture permeability of 50000mD (fracture conductivity of 500mD.m). To validate this point, simulations were carried out for different combinations of fracture width and fracture permeability keeping

the fracture conductivity as constant. For the simulations, the fracture conductivity of 500mD.m is used as shown in Table 2.3.

AARE with respect to the first simulation are 0.0010, 0.0017, 0.0017, and 0.0021 for simulations 2, 3, 4, and 5, respectively. As a result, it was confirmed that the change in fracture width or fracture permeability, keeping the fracture conductivity as a constant, does not affect the temperature decline curve over time (see Figure 2.10). Moreover, it does not affect the simulation time either. However, when the fracture size is chosen to be large enough, it does affect the results because the whole fracture acts like a coarse grid and creates discrepancies. Though this problem can be tackled by introducing refined grids within the fractures, this would increase the simulation time. Therefore, it is better to avoid wider fractures and choose a smaller fracture width with increased permeability, and this would give the same results as the previous case, provided the fracture conductivity is kept constant.

2.7 Proposed Model

To study the performance of an EGS in terms of temperature decline over time or energy extracted over time requires us to simulate the entire reservoir, which consists of huge number of grid blocks in all the directions. This would take a huge amount of time to build and run, even with high computational capability. On the other hand, reduction in the number of grids would have inaccurate results as discussed in earlier sections. As multiple simulations are required to study the effects of different parameters, it would become quite time consuming to do the simulations this way.

2.7.1 Reservoir Model

A better approach to this problem is by simulating one or two small sections (depending on the inclination of wells) of the entire model and then performing an analysis to upscale it based on the obtained results, to get the results for the entire reservoir. This would save time and would not require much computational capability. The entire reservoir is 500m along the x-axis, 400m along the y-axis, and the height of the reservoir along the z-axis depends on the inclination of the well and well spacing (maximum for 45 degrees and minimum for 90 degree). In order to have comparative models, the location and temperature of the last fracture (bottom-most) in the injection well were fixed and other parameters were varied as needed to get different models with different angle, fracture spacing, and well spacing.

In the proposed model, two fracture zones, namely the top two fractures or fracture number 1 and 2, and bottom two fractures or (n-1) and nth fractures, are simulated separately instead of simulating all n fractures as shown in Figure 2.11.

2.7.2 Simplified Model

According to the proposed model, the temperatures obtained from two simulations as shown in Figure 2.11 are used to represent the entire reservoir according to Equation 2.1

$$\bar{T}(t) = \frac{1}{2}\left(T_{1,2}(t) + T_{n-1,n}(t)\right) \qquad (2.1)$$

In the Equation 2.1, $\bar{T}(t)$ is the temperature of the fluid calculated by the proposed model at a particular time t. $T_{1,2}(t)$ and $T_{n-1,n}(t)$ represent the temperature of the fluid obtained from the simulation for the top and bottom two fractures, respectively, at the time t. This equation holds true for any reservoir that has a uniform temperature gradient

(linearly varying temperature) along the depth of the reservoir. If the temperature gradient is linear, the rate of heat extraction also varies linearly with depth. Therefore, when both the end points (top and bottom) are considered, the difference in the rate of heat extraction due to difference in temperature is taken into account, allowing us to predict the temperature decline curve for the entire reservoir by simulating two end points. Temperature decline curves from proposed models are shown in Figure 2.12.

The reason that two fractures were chosen instead of one was to capture the thermal interaction between two fractures. Top two fractures and bottom two fractures were chosen to develop the model because these two zones have the largest temperature difference and as the rate of heat extraction between the fluid and reservoir mainly depends on the temperature difference, both zones will have a different heat extraction profile and different decline curve (the temperature difference between two curves keeps decreasing; see Figure 2.12).

2.7.3 Simulation Design

To establish the robustness of the proposed model, a wide range of important factors, namely well inclination, well spacing, and fracture spacing, in geothermal systems are selected as shown in Table 2.4. Three levels of each parameter are chosen with Box-Behnken design of experiment method to reduce the total number of simulations. A total of 13 simulations are conducted as shown in Table 2.5. The properties mentioned in Table 2.6 are kept the same for all simulations. The dimensions of the entire model of the reservoir and its corresponding proposed model are mentioned in Table 2.7.

The height of the reservoir was varied so as to incorporate different inclination and

well spacing for the system. The dimensions of fractures were also varied in the z-direction so as to make sure the two wells are connected with the fracture plane. The height of the fracture (along the z-direction) was calculated as two times the well spacing.

In case of horizontal wells, simulation of only one fracture zone at the toe of the well was sufficient to get the decline curve for the entire reservoir, because all the fractures are identical and reside in the same temperature zone, whereas for the inclined well, two zones are needed as all fractures reside in a different temperature range.

2.8 Results and Discussion

The simulations were run for the entire model and also for the proposed model to study the differences between the two. The time to run the entire model and time for the proposed model are recorded for comparison. Average absolute relative error (AARE) and coefficient of determination (R^2) are calculated for error analysis.

Before discussing the results quantitatively, qualitative comparisons with the proposed model are shown in Figure 2.13. Spatial distributions of temperature on the x-y plane from the proposed model and the entire reservoir after a certain time are shown in Figure 2.13. It is clear from Figure 2.13 (a) that fractures do not interfere, i.e., two hydraulic fractures do not compete for heat extraction from the same region after 10 years. This phenomenon is also captured in both proposed simulations of the bottom and top two fractures. Similarly, fracture interferences are prominent after 30 years of heat extraction, which is clearly exhibited in the proposed model.

Quantitative comparisons of the proposed model and the entire reservoir model are shown in Table 2.8. The total numbers of grid blocks in the proposed model are less than

the grids required in the entire reservoir model. In case of well inclinations of 45 degrees and 60 degrees, the total time to run the two simulations (for top and bottom) in the proposed model took less time than to run the entire model. For the horizontal wells, only one simulation of the proposed model was run and the time was even less.

Decline curves of produced water temperature and relative errors between the proposed model and the entire reservoir model for various scenarios as described in Table 2.8 are shown in Figure 2.14. To maintain the baseline, the flow rate of 100 m^3/day/fracture was maintained in all cases for the proposed model and the entire reservoir. Figure 2.14 (a), (c), and (e) show the temperature decline curve for the production of heat from the EGS, over 30 years. The solid line represents the decline curve for the entire reservoir, whereas the dotted line is a result of calculations obtained from the proposed model. Figure 2.14 (b), (d), and (f) show the error percentage for the proposed model in comparison to the entire reservoir simulation, over 30 years. The graphs were grouped together on the basis of their inclination to get a better understanding of the performance of the proposed model with fractures in different temperature zones. It was observed that the proposed model for the EGS system, where only one/two fracture zone (consisting of two fractures) were simulated, gave accurate results throughout the life of the well with a maximum deviation of 2 to 3 degrees Celsius from the actual simulation, for the temperature decline curve. In almost all the cases, the temperature decline profiles of proposed models overlapped on the entire reservoir model. The error analysis showed that the relative errors are near to zero except for a few cases where the relative error is less than 3%. The R^2 values were observed to be close to one and the AARE values were less than 3%. As shown in Table 2.8, the proposed model was able to save a huge amount of time by reducing the

simulation time by 1.47-14.57 times for the given reservoir size. As our main purpose of running the thermal simulations for an EGS is to get an estimate temperature decline curve by studying the effect of various parameters, the proposed model serves as an excellent tool to do so in an efficient manner.

Also, a significant reduction in time was observed at a cost of insignificant error. As the chosen reservoir size was just 500m long (along x-axis), this model would be even more time efficient for evaluating large reservoirs. This shows that the proposed model for the entire reservoir gives promising results, and is flexible enough to be applied to any doublet model at any inclination, fracture spacing, and well spacing, with negligible errors. This implies that the proposed model can be used to obtain the temperature decline curve without actually simulating the entire reservoir.

2.9 Conclusion

This study focuses on the need for better, more time efficient simulation of a doublet model for an EGS. Coarse grids give inaccurate results in less time and finer grids gives accurate results with more time. Choosing the optimum grid size with fine refinements near dynamic areas for the simulation is really important to obtain proper results that are more accurate, and also time efficient. To know how much finer is going to give the best results in the least amount of time, it is better to start simulating a small portion of the reservoir with coarse grids and keep going finer until very few discrepancies in the results are obtained, and the results start to converge. The direction along the well, and perpendicular to the fractures, is least sensitive to the size of grids, but the plane of fracture is very sensitive, because of the fluid flow in the fractures.

While simulating planar vertical fractures for a reservoir, the fracture width and permeability of the fracture together decides the temperature decline curve, and their product together is called the fracture conductivity. When the fracture conductivity and fracture width are fixed, the permeability is automatically decided. Therefore, when highly conductive fractures are required, it is advised to keep fracture width low (1mm - 10mm) so that while modeling the system, the refinements near the fractures can be defined properly to avoid any discrepancies.

The proposed model for the doublet system of simulating the top and bottom zones of the entire reservoir can help analyze the temperature decline curve for the whole reservoir without simulating it. The results obtained this way are highly accurate (0-3% error) and 50-1000% more time efficient. The model is robust and can be used for any well spacing, fracture spacing, and for the wells at any angular orientation.

EGS is a fairly new topic and is expected to be in demand soon with the need of better power generation systems, as it has a reduced carbon footprint. This proposed model would be extremely useful when large numbers of simulations are to be carried out for a particular EGS to study, and optimized to get the most efficient system. It would save a lot of time in running simulations and give more time to analyze them. Hence, our new study would focus on the design and optimization of an EGS by manipulating five variables including well spacing, fracture spacing, angle of well, injection temperature, and flow rate, to obtain the most efficient system to generate electricity.

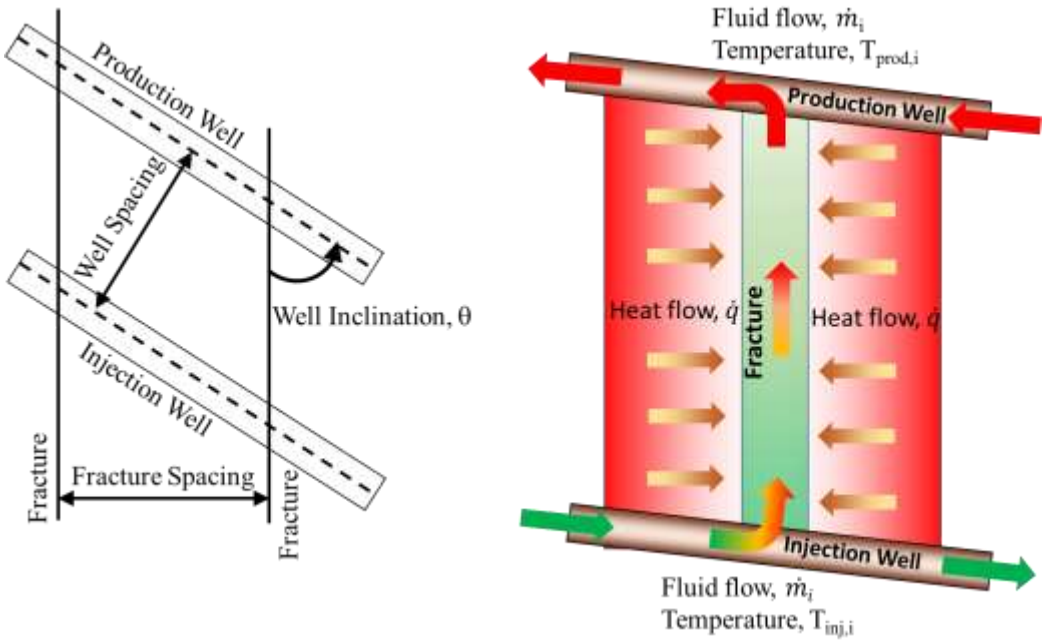

Figure 2.1: Representation of wells and fracture in 2D plane.

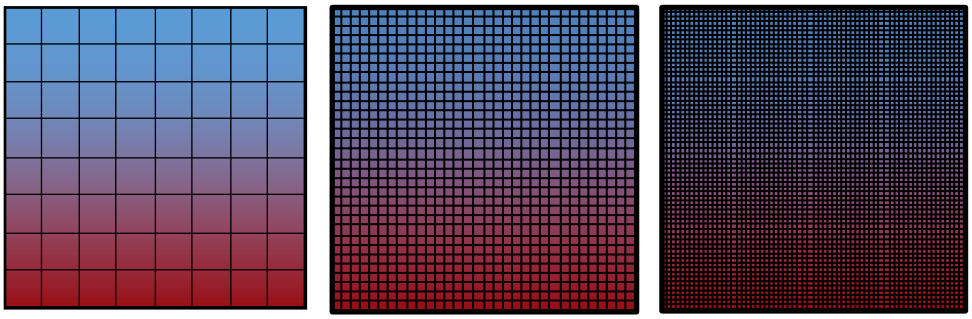

Figure 2.2: Different grid size from coarse to fine in x-z plane.

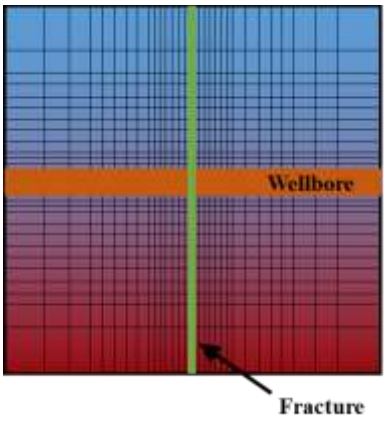

Figure 2.3: Variation in grid size from near fracture to away from fracture.

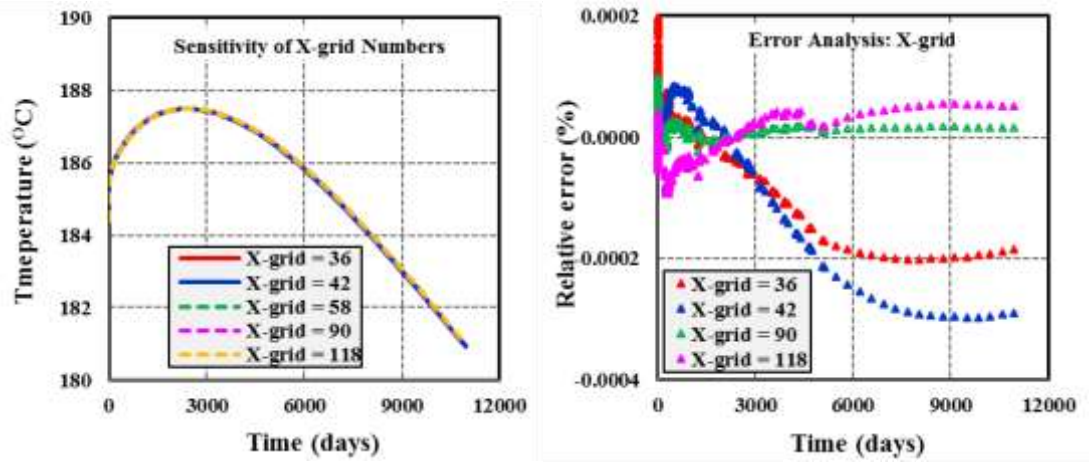

(a) (b)

Figure 2.4: Effect of different grid sizes in x-direction on (a) temperature of produced water with time (b) error in comparison to the base case.

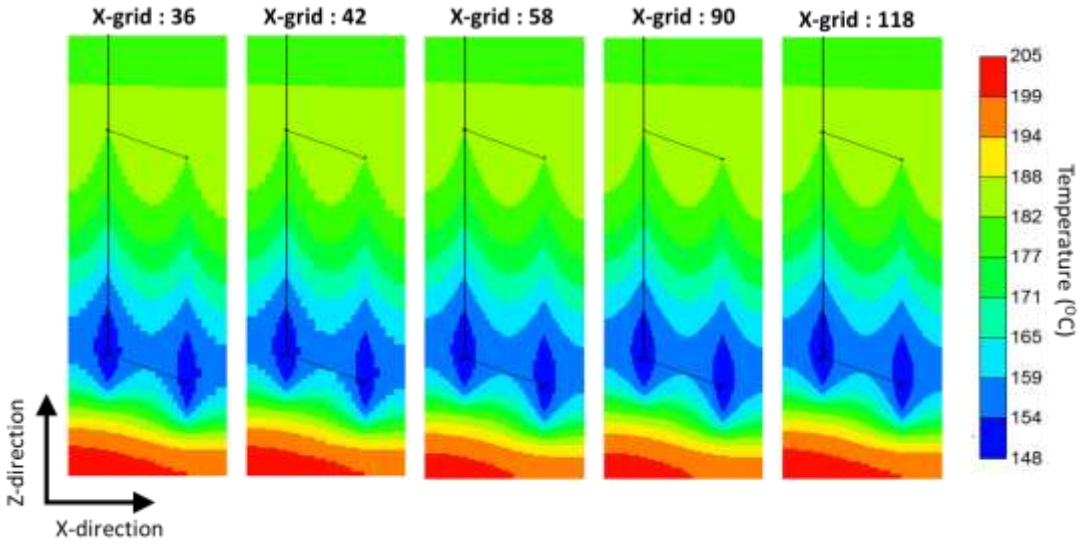

Figure 2.5: Spatial distributions of temperature on x-z plane with different numbers of grid in x-direction after 20 years.

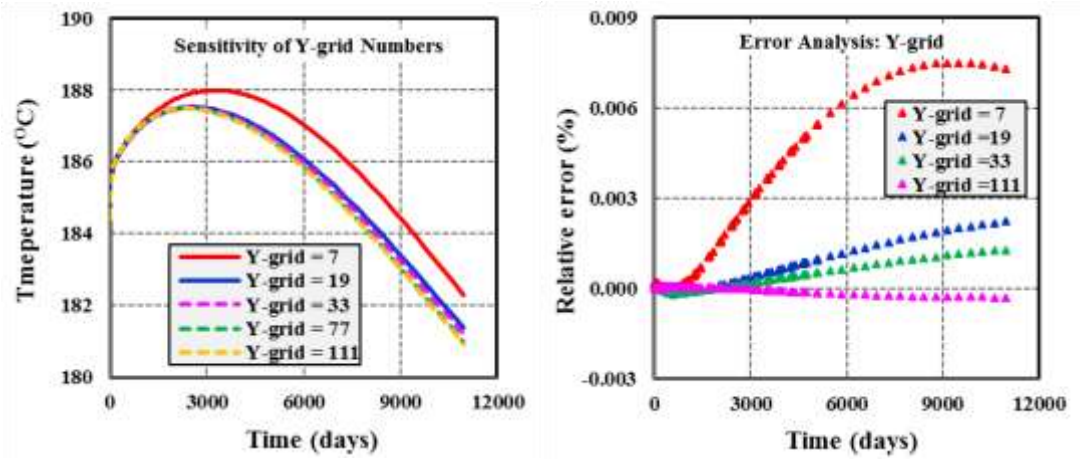

(a) (b)

Figure 2.6: Effect of different grid sizes in y-direction on (a) temperature of produced water with time (b) error in comparison to the base case.

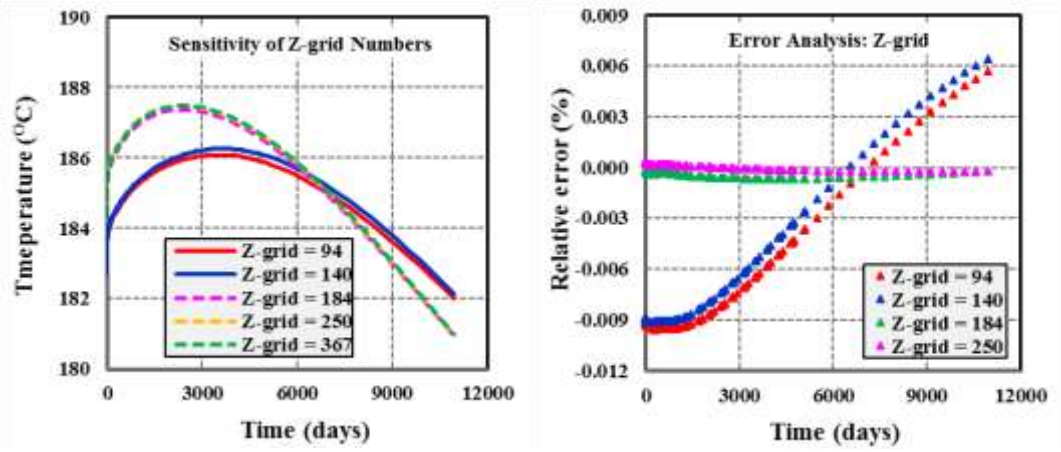

(a) (b)

Figure 2.7: Effect of different grid sizes in z-direction on (a) temperature of produced water with time (b) error in comparison to the base case.

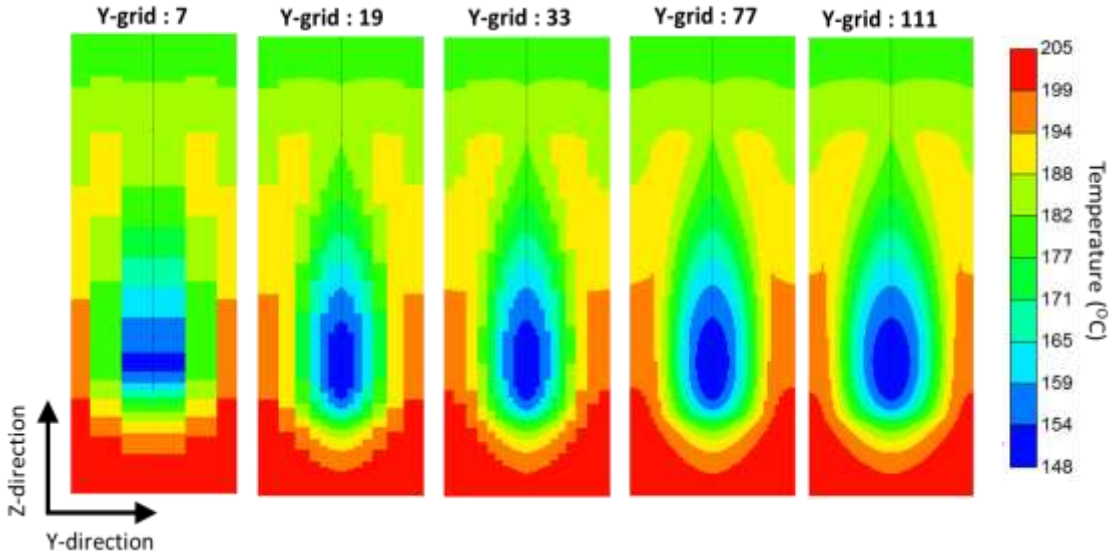

Figure 2.8: Spatial distributions of temperature on y-z plane with different numbers of grid in y-direction after 20 years.

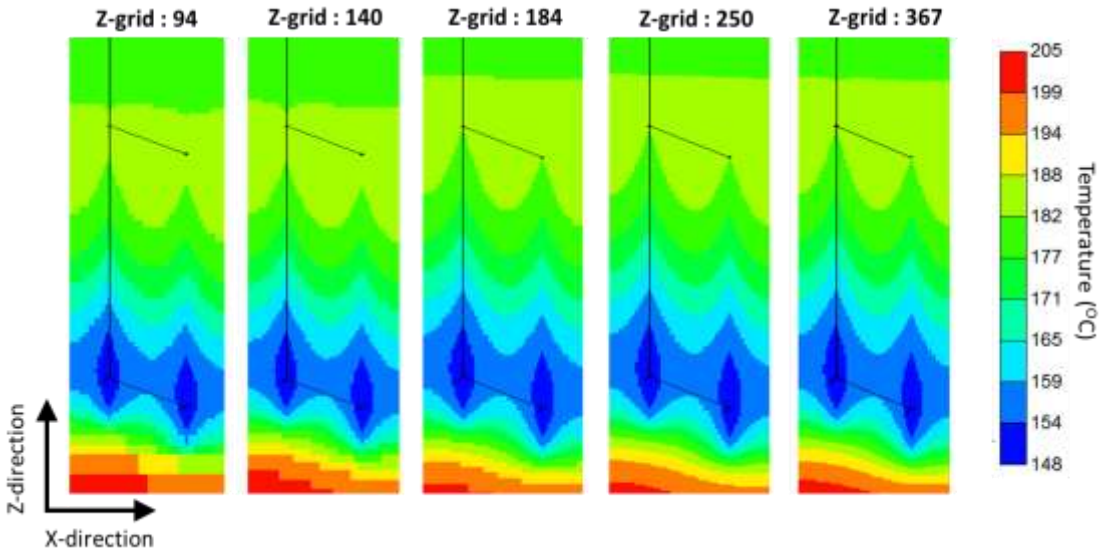

Figure 2.9: Spatial distributions of temperature on x-z plane with different numbers of grid in z-direction after 20 years.

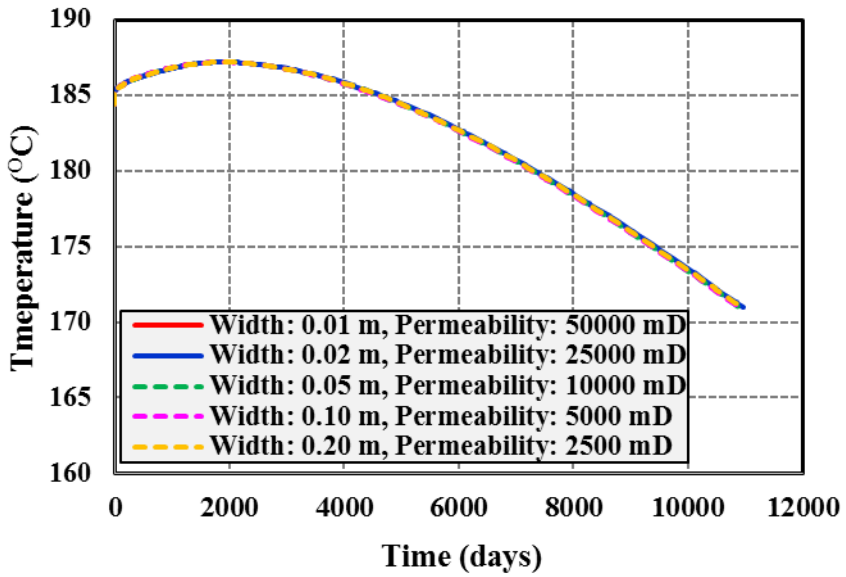

Figure 2.10: Temperature of produced water for different combinations of fracture width and fracture permeability with same conductivity.

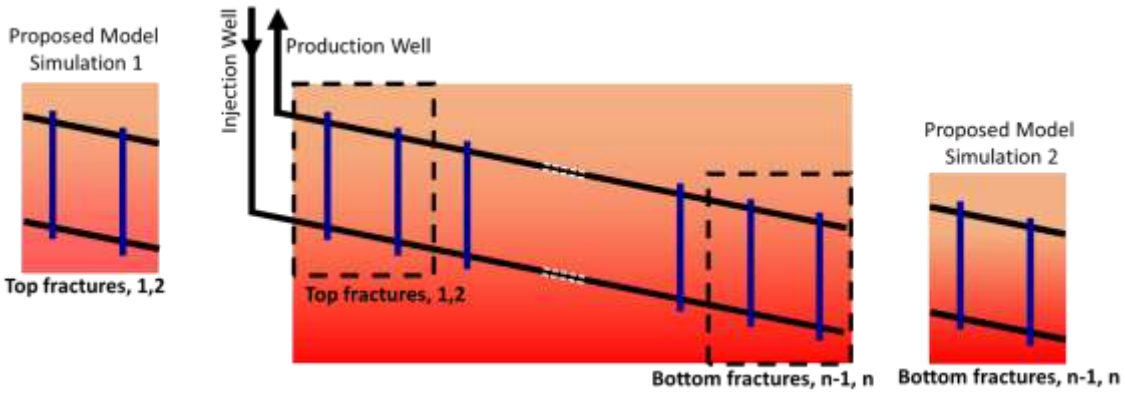

Figure 2.11: Schematic diagram of the proposed model: top two fractures on the left (first simulation of proposed model), entire reservoir in the middle, and bottom two fractures on the right (2nd simulation of proposed model).

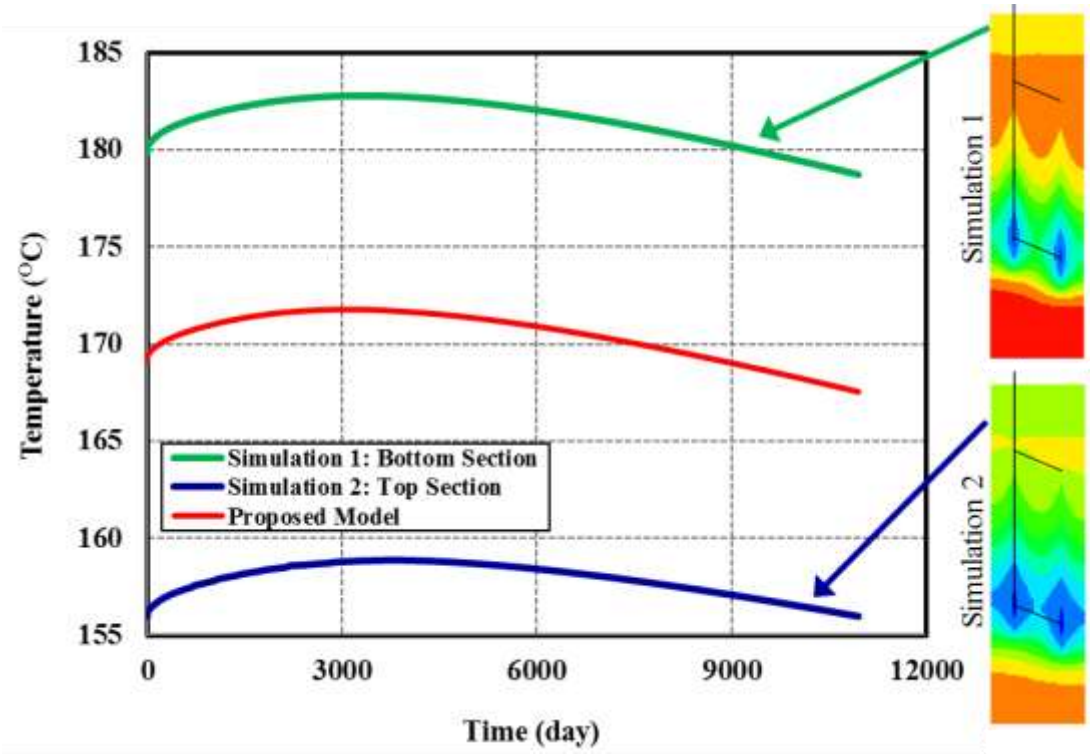

Figure 2.12: Temperature decline curve for top and bottom zone of the reservoir along with the entire model.

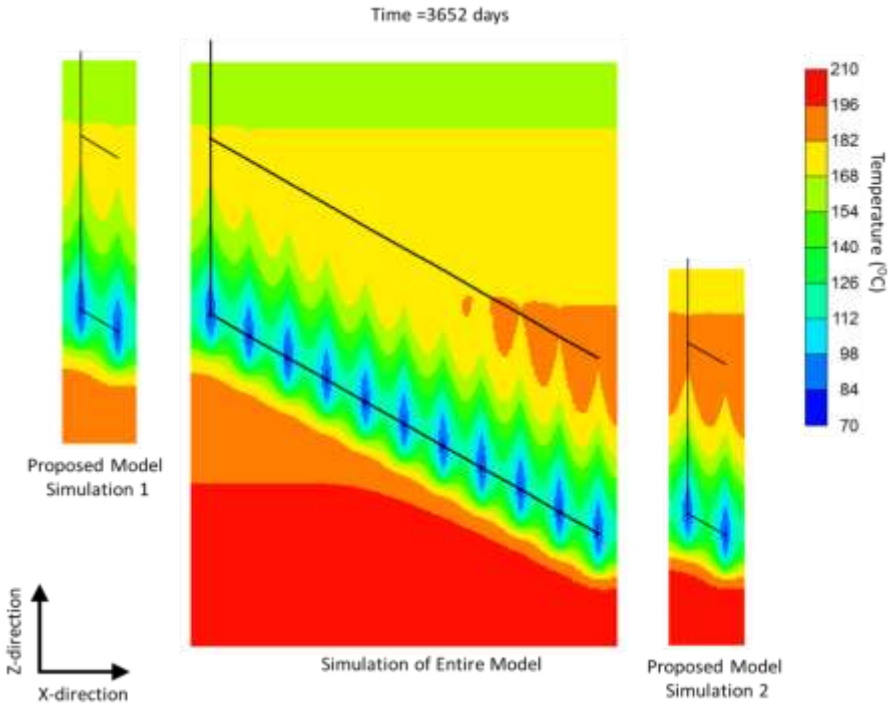

(a)

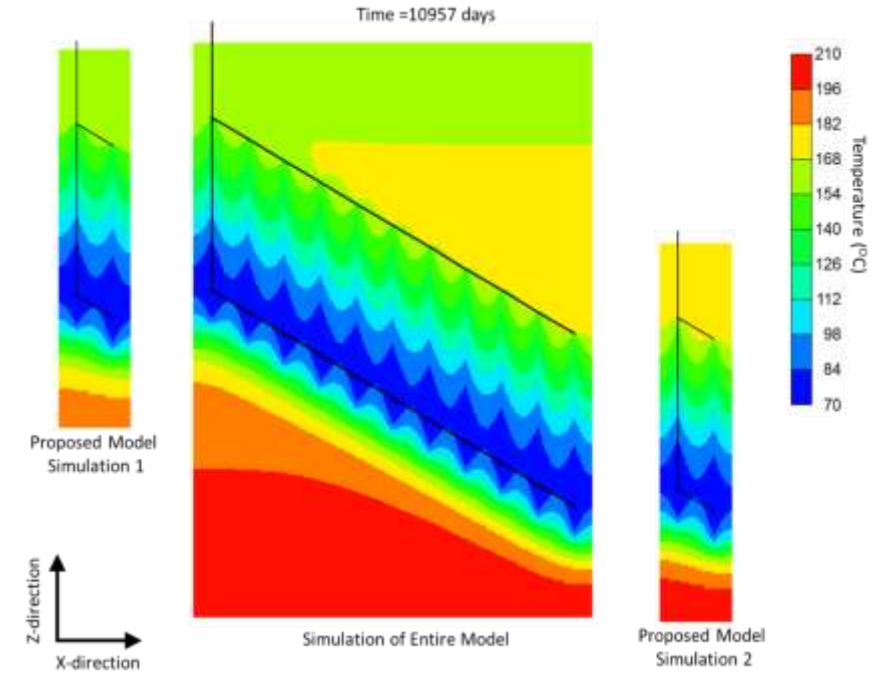

(b)

Figure 2.13: Comparison of spatial distributions of temperature among simulation of top two fractures in the left (part of proposed model), simulation of entire field, and simulation of bottom two fractures in the right (part of proposed model), after time (a) 3652 days (b) 10957 days.

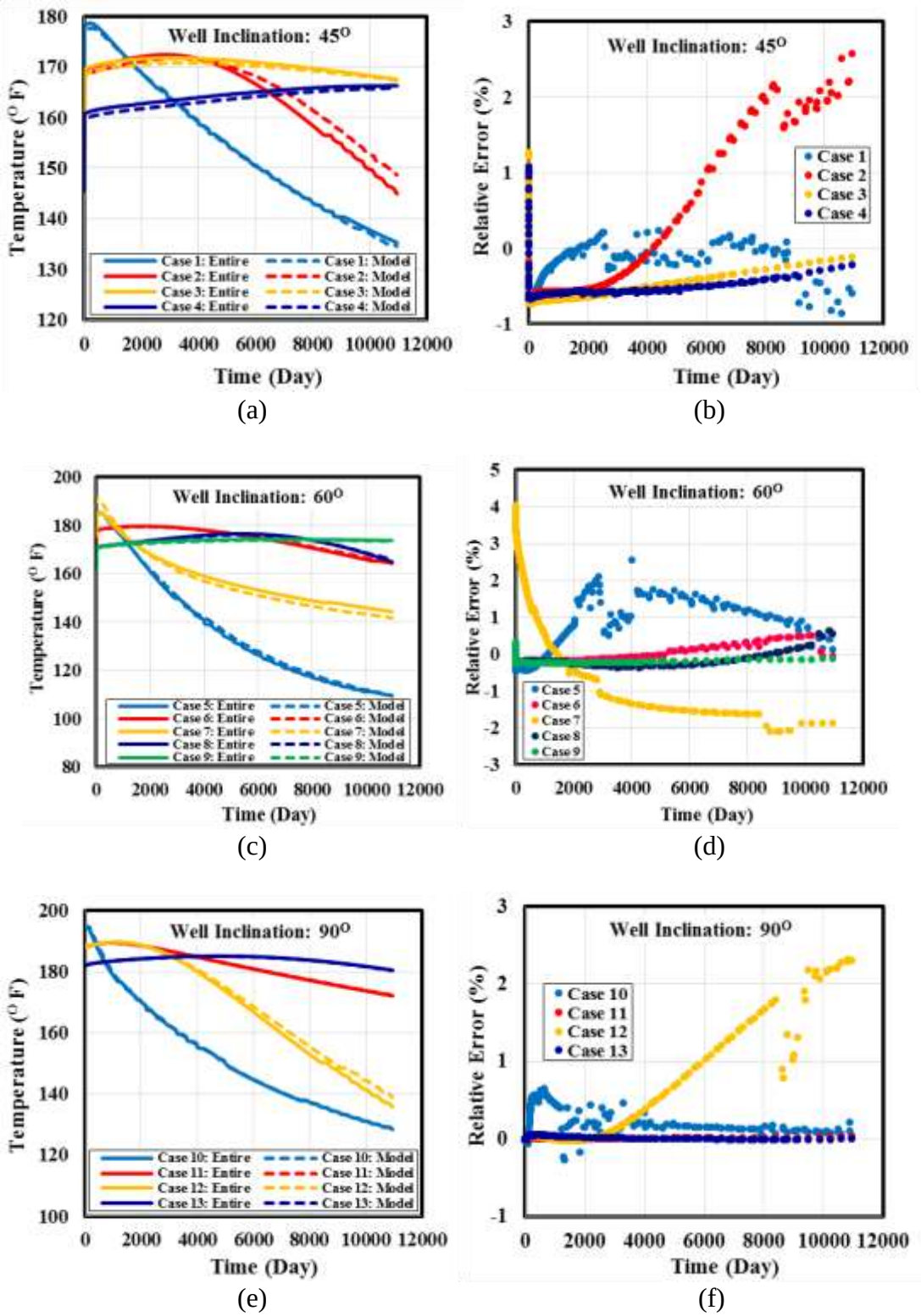

Figure 2.14: Comparison of proposed models for different well inclination angles; (a) & (b) are at 45 degrees, (c) & (d) are at 60 degrees, and (e) & (f) are at 90 degrees.

Table 2.1: Grid sensitivity in x, y, and z directions

Refinement Sensitivity	Simulation Number	Number of Grids in x-direction	Number of Grids in y-direction	Number of Grids in z-direction
Sensitivity in X-direction	1	36	77	367
	2	42	77	367
	3	58	77	367
	4	90	77	367
	5	118	77	367
Sensitivity in Y-direction	6	58	7	367
	7	58	19	367
	8	58	33	367
	3	58	77	367
	9	58	111	367
Sensitivity in Z-direction	10	58	77	94
	11	58	77	140
	12	58	77	184
	13	58	77	250
	3	58	77	367

Table 2.2: AARE in temperature of produced water between two consecutive grid systems

	Simulation Number	AARE (%) with respect to base Case 3
X -grid	1	0.731
	2	0.002
	4	0.002
	5	0.003
Y-grid	6	0.048
	7	0.008
	8	0.005
	9	0.001
Z-grid	10	0.893
	11	0.870
	12	0.034
	13	0.018

Table 2.3: Fracture conductivity

Simulation Number	Fracture width (m)	Fracture Permeability (mD)	Fracture Conductivity (mD.m)
1	0.01	50000	500
2	0.02	25000	500
3	0.05	10000	500
4	0.10	5000	500
5	0.20	2500	500

Table 2.4: Variable parameters

Sr. no	Parameters	Maximum (+1)	Medium (0)	Minimum (-1)
1	Well Inclination (degree)	90	60	45
2	Well Spacing (m)	300	200	100
3	Fracture Spacing (m)	100	50	25

Table 2.5: Box-Behnken design of experiments for three parameters

Case	Well Inclination (degree)	Well Spacing (m)	Fracture Spacing (m)
1	45	100	50
2	45	200	25
3	45	200	100
4	45	300	50
5	60	100	25
6	60	200	50
7	60	100	100
8	60	300	25
9	60	300	100
10	90	100	50
11	90	200	100
12	90	200	25
13	90	300	50

Table 2.6: Physical properties of formation, fracture, and fluid

Parameter	Value
Density of the rock, kg/m^3	2700
Permeability of the formation, mD	0.01
Permeability of the fractured zone, mD	50000
Porosity of the formation	0.01
Porosity of the fractured zone, %	10
Water Saturation, %	100
Thermal conductivity of formation, J/(m.day.℃)	2.592×10^5
Thermal conductivity of water, J/(m.day.℃)	5.18×10^4
Volumetric heat capacity of the formation, $J/(m^3.℃)$	2.133×10^6
Specific heat capacity of the fluid, J/(kg.℃)	4818
Formation compressibility, 1/kPa	4.4×10^{-7}
Temperature gradient, ℃/m	0.06
Reference depth, m	2520
Reference temperature, ℃	200
Injection Temperature, ℃	80
Injection Flow Rate, $m^3/day/fracture$	100

Table 2.7: Comparison of dimensions of entire reservoir model and proposed model

Dimensions	Entire Reservoir	Proposed Model
Reservoir length (X-direction), m	500	2 X Fracture spacing
Reservoir width (Y-direction), m	400	400
Reservoir height (Z-direction), m	Depends on well inclination and well spacing	Depends on well inclination and well spacing
Fracture width, m	0.01	0.01
Fracture half length, m		150
Fracture height, m	200-600 (Depends on well inclination and well spacing)	200-600 (Depends on well inclination and well spacing)

Table 2.8: Comparison of entire reservoir model and proposed simplified model

Sim No.	Total Grids		Simulation Run Time (hrs.)			Error Analysis in Temperature	
	Entire Reservoir	Proposed Model	Entire Reservoir	Proposed Model	Improvement Factor	R^2	AARE (%)
1	10927224	969892	12.0	3	4.00	1.00	0.51
2	19377512	772079	61.2	4.2	14.57	0.97	0.70
3	9281580	1794870	12.1	7.1	1.70	0.96	0.67
4	15491476	1955261	20.3	6.4	3.17	1.00	0.62
5	11235455	444444	18.9	2.3	8.22	1.00	0.35
6	11286968	1289750	13.5	4.5	3.00	1.00	0.21
7	5093550	964810	6.8	2.9	2.34	0.99	2.51
8	17568166	917378	34.9	6.1	5.72	0.99	0.21
9	8117340	2490180	11.0	7.5	1.47	1.00	0.22
10	2967888	680988	3.7	1.5	2.47	1.00	0.16
11	3751440	1250480	5.0	2.3	2.17	1.00	0.00
12	6099247	595441	11.9	1.8	6.61	1.00	0.21
13	6340488	1454838	8.8	2.7	3.26	1.00	0.02

2.10 Appendix

Among many error analysis techniques to evaluate the accuracy of models, coefficient of determination (R^2), relative error (RE), and absolute average relative error (AARE) are selected in this study. The coefficient of determination, R^2, indicates the overall accuracy of a model considering the two residual errors: error between model values and observed values and error between model values and average observed values as shown in Equation 2.2,

$$R^2 = 1 - \frac{\sum_{i=1}^{n}\left(Y_{obs,i} - Y_{model,i}\right)^2}{\sum_{i=1}^{n}\left(\bar{Y}_{obs} - Y_{model,i}\right)^2} \qquad (2.2)$$

The values of R^2 varies from 0 to 1. The values closed to unity are indication of the better fit of the model curve with observed data.

Absolute values of errors sometimes do not provide sufficient information about how large the errors are. To avoid this pitfall, relative error is measured at a particular point of a curve as shown in Equation 2.3.

$$RE(\%) = \frac{y_{i,obj} - y_{i,model}}{y_{i,obj}} \; X100 \qquad (2.3)$$

Relative errors show the error in each point of a curve with respect to that particular point. To calculate an overall error of the model, a single valued error is needed, which is absolute average relative error as shown in Equation 2.4.

$$AARE = \frac{1}{N}\sum_{i=1}^{N}\left|\frac{y_{i,\text{obj}} - y_{i,\text{model}}}{y_{i,\text{obj}}}\right| \text{X100} \qquad (2.4)$$

Use of absolute values are of interest to avoid any nullification of positive and negative errors.

2.11 References

[1] M.C. Smith, R.L. Aamodt, R.M. Potter, and D. W. Brown. (1975). Manmade Geothermal Reservoirs, LA-UR-75-953.CONF-750525-6. New Mexico, USA: Los Alamos Scientific Laboratory.

[2] J.W. Tester, D.W. Brown, and R. M. Potter. (1989). Hot Dry Rock Geothermal Energy – a New Energy Agenda for the 21st Century, LA-11514-MS New Mexico, USA Los Alamos National Laboratory.

[3] D. Duchane, and D. Brown. (2002). Hot Dry Rock (HDR) Geothermal Energy Research and Development at Fenton Hill, New Mexico Geothermal Heat Center Bulletin.

[4] A. S. Batchelor (1985), Progress in hot dry rock exploitation. Int. J. Energy Res., 9: 377–390. doi:10.1002/er.4440090312.

[5] F. H. Cornet (1989). Experimental investigations of forced fluid flow through a granite rock mass. Paper presented at the Proceedings of 4th International Seminar on the Results of EC Geothermal Energy Demonstration, April 27-30, Florence, Italy.

[6] Department of Energy, USA. (2008). An Evaluation of Enhanced Geothermal Systems Technology: Geothermal Technologies Program.

[7] Y. Xia, M. Plummer, E. Mattson, R. Podgorney and A. Ghassemi. (2017). Design, modeling, and evaluation of a doublet heat extraction model in enhanced geothermal systems. Renewable Energy, 105, 232-247. doi: 10.1016/j.renene.2016.12.064

[8] Y.C. Zeng, Z. Su, and N.Y. Wu. (2013). Numerical simulation of heat production potential from hot dry rock by water circulating through two horizontal wells at Desert Peak geothermal field. Energy, 56, 92-107. doi: 10.1016/j.energy.2013.04.055

[9] W. Huang, W. Cao, and F. Jiang. (2017). Heat extraction performance of EGS with heterogeneous reservoir: A numerical evaluation. International Journal of Heat and Mass Transfer, 108, 645-657. doi: 10.1016/j.ijheatmasstransfer.2016.12.037

[10] P. Panja, T. Conner, and M. Deo. (2013). Grid sensitivity studies in hydraulically fractured low permeability reservoirs. Journal of Petroleum Science and Engineering, 112, 78-87. doi: 10.1016/j.petrol.2013.10.009

CHAPTER 3

PERFORMANCE EVALUATION OF ENHANCED GEOTHERMAL SYSTEM (EGS): SURROGATE MODELS, SENSITIVITY STUDY, AND RANKING KEY PARAMETERS[2]

3.1 Abstract

Designing an efficient system to extract heat from an EGS requires proper understanding of the behavior of the geothermal reservoir over a long period. Five key parameters, namely well spacing, fracture spacing, well inclination angle, injection temperature, and injection rate, are considered in this study for a doublet well system. These are in addition to the reservoir temperature and other reservoir attributes. To study and evaluate the performance of an EGS, second order surrogate models for 'produced water temperature', at certain time intervals are developed as a function of these five factors. These models also capture the effect of the interactions among the mentioned parameters up to second order. The in-situ properties of a candidate reservoir for designing the simulations are taken from the FORGE site, Utah. Simulations are designed using 'Box-Behnken' design of experiment techniques to minimize the number of simulation cases. The models are trained and tested with the simulated results from the Utah FORGE

2 Pranay Asai, University of Utah; Palash Panja, University of Utah; John McLennan, University of Utah; Joseph Moore, University of Utah

geothermal reservoir. Fitness of the models is calculated by estimating the errors using the coefficient of determination (R^2) and the normalized root mean square error (NRMSE). These surrogate models would be used to study the sensitivity of the aforementioned factors on the temperature of the produced water and the heat recovery over a time period of 30 years. Finally, the hierarchy of factors, as they impact the total heat recovery, are represented as a tornado plot. Heat recovery is directly proportional to well spacing as more well spacing would contain a large volume of the reservoir from which to extract heat. Injection temperature is in second place in the hierarchy of relevance. The well inclination angle, within the studied range, had the least impact on heat recovery compared others. This study is helpful for proper planning, designing, and development of an enhanced geothermal system.

3.2 Introduction

Geothermal energy has been studied since the early 1900s [1-3]. Geothermal reservoirs, also known as hot dry rock [4, 5], have potential to be a great source of energy. A good geothermal system usually should have three key properties: high temperature reservoir (200+°C), highly conductive natural fracture system, and availability of a working fluid to bring that heat to the surface. Usually it is possible to find high temperature reservoirs (at economically accessible depths), but the possibility of finding a highly conductive fracture system in such reservoirs is less likely. The development of Enhanced Geothermal System (EGS) has been visualized as a breakthrough because it only relies on the availability of high temperature reservoirs. It conceptually consists of drilling two or more parallel or near parallel wells (a few hundred meters apart, for example). These are

connected by developing a network of hydraulic fractures in the reservoir, hence eliminating the requirement of a naturally occurring fracture system. One or multiple wells can be used to inject the working fluid (usually water) into the reservoir (via hydraulic fractures exiting the injection wells), allowing the fluid to extract the heat. This heated fluid is produced from the remaining wells (production wells). The network of fractures plays an important role because it increases the surface area inside the reservoir that is used to enhance the heat transfer rate from the reservoir to the working fluid.

Creating an efficient EGS is a major challenge faced by the industry. It requires a huge capital investment [4] and hence calls for the proper planning, design, and development of the system. It is important to have a better understanding of the key parameters and their effect on the performance of the EGS. A good EGS system should be able to generate sufficient heat to produce electricity and should be sustainable for at least 30 years. One way to ensure proper planning of an EGS is by carrying out simulations to emulate the reservoir and then trying out various combinations of the five key parameters to enhance the performance. Unfortunately, this method could take quite a long time since all of the possible combinations would have to be evaluated before choosing the best one. To get around this problem it is feasible to study the impact of individual parameters and rank them and then use this to optimize the design program. This would help develop an efficient system in less time.

There have been many studies to assess the impact of various parameters involved in development of an EGS. There have been studies focusing on different type, of EGS to evaluate their performance. Sanyal et al. [5] studied a five-spot layout of a 3D EGS model (hypothetical) with one injection and four production wells. They analyzed their optimal

performance on the basis of fracture spacing, reservoir permeability, and well geometry. Frash et al. [6] carried out studies on drilling doublet and triplet well systems (a triplet is one injector and two producer wells). They mentioned the importance of proper well trajectories to ensure that the wells intercept the hydraulic fractures to allow the fluid to be circulated. Studies that emphasize the effect of individual parameters on EGS performance include the work of Sun et al. [7] and Cao et al. [10]. Sun et al. evaluated the effect of different fracture geometries on heat extraction from the reservoir. Cao et al. studied the effect of carrier fluid on the heat extraction. Other studies that have been carried out also include the simultaneous effects of two or more parameters. Xia et al. [8] performed a sensitivity study on fracture spacing, deviation angle of the parallel wells, and injection flow rates. Aliyu et al. [9] considered the effects of injection flow rate, fluid injection temperature, and lateral well spacing. Although these studies do help to understand the importance of choosing the right values for the given parameters, they do not tell much about how much a particular parameter affects the performance of the EGS.

The objective of this study is not only to determine the key factors that affect the efficiency of the EGS, but also to determine the effect of each individual parameter. The effect of each parameter on the total heat extraction would also be studied. A step-wise approach to developing a high performance EGS is also discussed. On the basis of the implementation stage in the EGS, the factors would be grouped into three categories: natural parameters, completion parameters, and operational parameters. The key factors that are analyzed and studied in this paper include well spacing, fracture spacing, well inclination, fluid injection temperature, and fluid flow rate. All of these factors were studied individually to determine their impact on the heat recovery efficiency of a typical

EGS over its lifetime.

3.3 Method of Energy Extraction

The Earth is a vast reservoir of heat source; the deeper we go, the higher the temperature gets. Drilling to excessive depths becomes increasingly expensive. It is preferable to choose sites that have high temperature reservoirs at relatively shallow depths. The temperature and the dimension of the reservoir will play an important role in deciding the heat capacity and life of the geothermal system. Two or more wells can be drilled into the reservoir, accessing this huge heat source, which would be subsequently connected by a network of hydraulic fractures. A fluid would be circulated in the system (which acts as a heat carrier), to extract the heat up to the surface. When this working fluid passes through the network of hydraulic fracture, it comes in contact with the hot rock, where it extracts heat via convection and conduction. The driving factor for transfer of heat is the temperature gradient between the reservoir and the fluid. As the temperature difference between the rock and fluid increases, the rate of heat transfer also increases. This implies that a cooler fluid would extract more heat than a warmer fluid in the same amount of time. In addition, the surface area of the fracture network plays an important role because it facilitates the interaction of the fluid with the hot reservoir rock. If the fracture network is widespread and has good conductivity, there would be an increased rate of heat transfer. Once the fluid comes back to the surface, a heat exchanger can be used to extract the heat from the fluid before reinjecting it into the system.

3.4 Enhanced Geothermal System (EGS)

EGS is a method of creating a fluid circulation system to extract the heat from the reservoir. An EGS is visualized to consist of an injection well, a production well, and multiple stages of hydraulic fractures (see Figure 3.1). The fracture network provides an interaction pathway for the fluid and the reservoir rock. It also connects the injection and production wells to complete the circuit. Many possible combinations can be used in an EGS to extract the heat from the reservoir. In this study, a simple doublet system is used, consisting of an injection well and a production well, connected by multiple hydraulic fractures along and orthogonal to the wells. The working fluid used here is water because it is generally available and has a high heat capacity. The whole system will operate in a closed loop with a make-up line to account for fluid losses in the reservoir. The water is pumped under high enough pressure to maintain its state as liquid, which proves beneficial as this eliminates any fluid losses that may occur during flashing of the liquid (to extract heat) and also saves time as the water does not have to be condensed before reinjecting.

The potential of any geothermal project can be determined by evaluating three parametric groups (categorized on the basis of their implementation stage), namely natural properties, completion parameters, and operational parameters.

Natural properties are intrinsic properties of the geothermal reservoir and is the first stage for development of EGS. These include the thermal gradient of the system, the heat capacity, thermal conductivity and density of the formation, size of the reservoir, and availability of natural fracture networks. As in-situ properties of a specific location, they cannot be readily manipulated or altered. These properties help to determine the total heat content of the reservoir and the facility for transferring heat to the working fluid. A good

geothermal reservoir has high temperature (200+°C) at shallow depths, high temperature gradient, high formation enthalpy, and high thermal conductivity.

The next step is to decide on the completion parameters that would help determine the type of EGS to be established to produce the energy from the geothermal reservoirs. These include the number of injection/production wells, type of well system (doublet, triplet, quadruplet etc.), angle of inclination of the wells, well spacing, and number of hydraulic fractures or fracture spacing. These factors are crucial; they control the contact area/volume in the reservoir. These will primarily control the total heat recovery factor for the EGS system. A system that has larger areal coverage in terms of fracture network would be more efficient in extracting heat from the entire reservoir.

The final stage is to decide on the operational parameters. They play an important role in heat recovery from the reservoir. These include the type of working fluid, the fluid flow rate, and the injection temperature. Once the recovery factor for the EGS is established by the completion parameters, operational factors will determine the rate of heat extraction and the life of the EGS. For example, a system with a high flow rate and low injection temperature will thermally deplete the reservoir faster than a system with low flow rate and high injection temperature.

Thus, in order to achieve better energy recovery, optimization of each individual group is extremely important. To optimize a system, it is necessary to study and evaluate the impact of each of these parametric groups by carrying out multiple simulations.

3.5 Simulation of EGS

To study the effect of different parameters on the efficiency of the EGS, multiple simulations need to be carried out to understand the effect of each factor individually. This study considers the effects caused by three completion parameters (wellbore inclination, well spacing, and hydraulic fracture spacing) and two operational parameters (flow rate and injection temperature) on the overall efficiency of the EGS.

A model was created using data from the FORGE (Frontier Observatory for Research in Geothermal Energy) site near Milford, Utah. The temperature gradient at the FORGE site is 60°C/km with a reference temperature approaching 200°C at a true vertical depth of 2500m. The site has low porosity (~**1**%) and low permeability (around 200μD to 1000μD) igneous rock (granite and granodiorite). Fluid flow and heat flow in an EGS with one fracture, one production well, and one injection well are shown in Figure 3.2.

The EGS at the Utah FORGE site would be a doublet system with two inclined wells (60° from the vertical). The injection well kicks off at the depth of 1460m and the perforations starts from 1910m and the toe of the well is at 2518m. This will provide a 1216m lateral injection zone that can be hydraulically fractured to circulate water through the reservoir. Another well (production well) will be drilled proximal to the injection well with the spacing (measured perpendicular to the well) of 200m. The production well will be located vertical above the injection well.

The data obtained from the FORGE site were used to prescribe natural factors in the simulations. The simulations used a commercially available thermal reservoir simulator, CMG STARS. The simulation model consists of a doublet with water as the working fluid. The wells were considered to be parallel. Well spacing, fracture spacing,

wellbore inclination, fluid injection rate, and injection temperature were varied to study their effect. Table 3.1 summarizes the dimensions of the reservoir that was modeled.

The hydraulic fractures in the model were simple planar fractures - rectangular shape and large enough surface area to emulate the hydraulic fractures. These consisted of grids with higher permeability and porosity than the surrounding reservoir, giving rise to highly conductive zones connecting the two wells. All of the simulated factures were assumed to be uniform and isotropic with the same fracture conductivity. The natural properties for the simulated model were taken from the FORGE site and are mentioned in Table 3.2.

3.6 Surrogate Model

The surrogate models to represent an entire reservoir in mathematical form were developed for the temperature of the produced water and consequently the total heat extraction as a function of time. One surrogate model represents temperature at a particular time for a set of inputs. It is not realistic to develop surrogate models for thousands of points on a temperature versus time profile. To avoid this complication, few selective times such as day 1, day 2, day 3, etc. are chosen for surrogate models. The values for intermediate time such as time between day 1 and day 2 or day 2 and day 3 are interpolated. The discretization method to obtain data from the time continuous results for the surrogate model are shown in Figure 3.3 with two example results.

The time interval depends on the nature of the curves. During the simulation, smaller time steps are considered near the curve with sharp changes such as time before 5 years. Few example points are shown in Figure 3.3. In this study, 59 time points were taken

over the entire operational time span of 0 to 30 years. As expected, increasing the number of times sampled over the 30 year plant life provides more accurate results, but the computational time increases proportionally. It is mentioned earlier that one surrogate model is developed for each chosen time and hence, 59 surrogate models were developed. The results for times that were not modeled are obtained by interpolation between the two consecutive time points (which were modeled). In this manner, the results for the entire time period were determined by interpolation and smoothing.

The nature of the temperature decline was not the same for all operating, completion, and natural parameters. For clarification, two different type of temperatures profiles obtained from simulation of EGS are shown in Figure 3.3. In one curve (red line), the decline is sharp from a very early time. On the other hand, in the second curve (blue line), the temperature increases and then decreases slowly. This difference in the nature of decline curve may have an effect on the surrogate model in that particular time frame.

A response surface model (RSM) using a second order polynomial function was developed and this is shown in Equation 3.1

$$\log(f(X_1, \dots, X_5)) = a_0 + \sum_{k=1}^{n} a_k X_k + \sum_{i=1}^{n} \sum_{j=i}^{n} a_{ij} X_i X_j \qquad (3.1)$$

In this model, second order interactions among variables are also considered. The number of coefficients depends on the number of independent variables. For 5 input variables, there are 5 coefficients, 'a_k', 15 second order interaction coefficients, 'a_{ij}' and one intercept, 'a_0', as shown in Equation 3.1. These 21 parameters are obtained for 59 models of the temperature of the produced water. All the coefficients and intercept are obtained from an in-built optimization routine in Matlab (Matworks Inc.) computer

programming platform. In the optimization method, the error between the model and the training data is minimized. To avoid any unexpected results predicted by the model (such as negative temperature), the common logarithm of the temperatures was taken before developing the surrogate models. Finally, results are obtained from the surrogate model by converting to the power of ten (in the case of a common logarithm that uses base 10) securing positive values.

The workflow for developing surrogate models is shown in Figure 3.4. It starts by determining the number of parameters or variables to study. Once that is decided, the next step is to design a set of experiments to study their impacts (in this study, Box-Behnken was used) by choosing a range of inputs. Other parameters (natural properties of the reservoir) are also taken into account to design the simulation. The data used to design the simulations are referred to as the training data. Using these data and the results from the simulations, a surrogate model is developed using multivariate regression. This is referred to as the initial model. After that, a randomly generated test data set (within the range of training data) is used to validate the developed model. If the test data are not able to validate the model, another surrogate model has to be developed using a different approach and different level of interaction. This process is repeated until a satisfactory model is developed.

3.6.1 Design of Experiments

This study emphasized five parameters. These were well spacing, fracture spacing, wellbore inclination, injection temperature, and total injection rate. To evaluate the effects of each individual parameter on the total heat extraction in EGS, an experiment was

designed using the Box-Behnken (Box and Behnken 1960) method. Box-Behnken uses a three-level model (maximum, medium, and minimum) to reduce the number of experiments and yet predicting accurate results for the experiment. For five variables (as shown in Table 3.3), 41 simulation models were designed, each having its maximum value (+1), medium value (0), and minimum value (-1). This method uses second degree and second order interactions, which is ideal for generating second order surface response models. All of the parameter's maximum, medium and minimum values were chosen linearly, except for the angle of well inclinations. As the well inclinations chosen for this study (45°, 60°, and 90°) are not linear, the inverse of angle was chosen to get linear values. All the values are then converted to +1, 0, and -1, using liner conversions.

The 41 simulations were used to train and develop a model that can produce results without actually running the simulations (considering the input values are within the maximum and minimum range). These 41 simulations are referred to as the training data. Apart from these, 10 other simulations were also designed with random values of inputs (within the maximum and minimum range), referred to as test data. The purpose of the test data is to validate the model produced using the training data. If the test data do not give a satisfactory result, the model is trained again using different sets of instruction to generate a new model. This step is repeated until the test data validate the trained model in satisfactory limits. The fitness of a model with training data and test data is discussed in the next section. The fitness is determined by two measures, the coefficient of determination (R^2) and the normalized root mean square error (NRMSE). Further details of the experiment design are summarized in Appendix A.

3.6.2 Training of the Model

Once the model is developed, the training data assists in evaluating the performance with the data obtained from the model. Since multiple models are created for an individual time, it is important to assess them and check for any discrepancies. The RSM surrogate model predicts the temperature decline curve for given sets of input. A comparison of the training data and the data obtained from the model is plotted in Figure 3.5. Figure 3.5 (a), includes the data points for the first day, first year, and the fifth year, and Figure 3.5 (b) includes the data points for the tenth, twentieth, and thirtieth years.

While the model shows a good fit with the training data, this does not necessarily validate the model because the model is created using the training data. To estimate the error for the generated model, the R^2 and NRMSE (Normalized Root Mean Square Error) are calculated and plotted in Figure 3.6. Figure 3.6 (a), shows the R^2 values for each of the 59 time-based models. It shows that all of the models have R^2 values close to 1. This indicates that the model has relatively small errors and does not deviate much from the training data. Figure 3.6 (b) shows the NRSME values for all of the 59 time-based models. Most of the time-based models have around 1% error, but there is an observable peak for a few of the models. This peak is the result of having different nature of temperature decline curves because of different well spacing, which leads to different temperature decline curve for produced water. Despite that, the model is well trained and can be used because the errors are in an acceptable range.

3.6.3 Testing of the Model

As the models were generated using the training data, they would replicate the results accurately with the exact same data set, but they might not be able to give good results with another data set chosen randomly within the range. To check the validity of the generated model, it is important to create a random data set (within the range of the training data set) and evaluate the performance of the trained model and compare it with the results from test data (see Figure 3.7). Usually 20% of the total data are used as test data to validate the model [10]. Figure 3.7 (a) shows a comparison of test data with the data obtained from the trained model, for the first day, first year, and fifth year. Figure 3.7 (b) shows the same comparison for tenth year, twentieth year, and thirtieth year. The test data show a poorer fit as compared to the training data. Despite that, the test data performed efficiently without any major discrepancies and hence validate the trained model.

The errors were calculated for the test data using R^2 and NRMSE, as shown in Figure 3.8. Figure 3.8 (a) shows the R^2 values for the test data and Figure 3.8 (b) shows the NRMSE values.

Except for a few time-based models, most of them have good R^2 values (close to 1) and less percentage of NRMSE. The discrepancies in the mid portion are again the result of the different nature of temperature decline curve. Overall, the test data show good results and hence successfully validate the trained model.

3.7 Results and Discussion

Results are discussed in terms of temperature decline and the total heat recovery over time. The study of temperature decline is important because if the system is connected

to a binary power plant, to produce electricity, it has certain limitations and cannot produce power below a certain temperature of produced water. Moreover, the lower the temperature, the lower the efficiency of the Organic Rankine Cycle plant. When the system starts producing water below this temperature, it either needs to be shut down or the surface equipment - such as the heat exchanger or other associated units - should be modified to work with this low temperature (which is not possible in a commercial scenario).

The heat recovery for the system with flow rate Q, fluid density ρ, fluid heat capacity C_p, injection temperature T_{inj}, and temperature of produced water T_p. over time period t is calculated using Equation 3.2. The influence of well spacing, fracture spacing, well inclination, injection temperature, and flow rate on the temperature of produced water and total heat recovery is discussed in the next sections.

$$Total\ Heat\ Extraction, H = \int_0^t Q\ \rho\ C_p\ (T_p - T_{inj})dt \qquad (3.2)$$

3.7.1 Well Spacing

Figure 3.9 (a) is a surface plot for temperature decline, obtained by simulating five well models at different well spacing, with 100m being the least and 300m being the maximum. All other parameters were kept at their medium values. It shows that when the well spacing is the least (100m), the temperature of produced water drops drastically in the initial 10 years and then it becomes less steep. When the well spacing is maximum (300 m), the temperature is quite stable and does not drop below 150°C. In Figure 3.9 (b), it is a representation of the total amount of heat extracted by the EGS over 30 years. For 300m well spacing, the heat extracted is almost three times more than that extracted by a system with 100m well spacing. This demonstrates the critical importance of well spacing.

Decline in total heat production is observed because the distance between the wells determines the primary coverage volume of the EGS. When the well spacing is reduced, the wells encompasses a smaller volume than they do when the spacing is greater. Since the volume of rock is directly proportional to the available heat content, the smaller volume of heated rock encompassed for 100m well spacing is depleted faster than the larger volume associated with a 300m well spacing; all other parameters being constant. Thus, well spacing determines the primary heat recovery factor for the given geothermal reservoir. Although this indicates that the well spacing should be maximized in order to achieve maximum recovery factor, this is usually restricted by physical limitations. As the well spacing increases, it becomes more difficult to connect the two wells with a regular fracture network. Hydraulic fracturing methods have some limitation in terms of connecting two wells, thus restricting the well spacing.

3.7.2 Fracture Spacing

Figure 3.10 (a) represents a temperature decline surface plot obtained by simulating five well models at different fracture spacing, from 50m to 100m (other parameters were kept at the medium values). The 50m fracture spacing gives a steady decline curve for the temperature than the 100m fracture spacing. Alternatively, Figure 3.10 (b) represents the cumulative heat extracted at variable fracture spacing over 30 years.

In EGS with fixed well lengths, lower fracture spacing implies more fractures and more fracture spacing would mean fewer fractures. It is advantageous to have smaller fracture spacing (more fractures) because this increases the surface area for rock-fluid interaction. Since the well spacing is already fixed, more fractures would lead to the

extraction of more heat in a shorter time. However, if the fracture spacing drops below a certain level, the interference would occur and this would negatively affect the EGS's performance.

3.7.3 Well Inclination

Figure 3.11 (a) represents the temperature decline surface plot obtained by simulating five well models at different well inclination angles, from 45° to 90° inclinations (other parameters were kept at medium values). It was observed that completely horizontal wells (90° to the vertical) perform better than the inclined wells (45°). Of more importance, the total heat extracted in 30 years is higher in the horizontal well; see Figure 3.11 (b).

When the two wells are horizontal, all of the fractures lie in the same temperature zone. When the wells are not horizontal, the fractures reside in different temperature zones (at different positions along the wells), hence producing water at different temperatures. Since the first fracture's location (located at the toe of the well) is kept fixed, in an inclined well system, the second last fracture would lie in a lower temperature zone. Thus, inclined wells would perform less efficiently than the horizontal wells. In addition, the volume of rock contained between two horizontal wells system would have a higher average temperature than the volume of rock contained between the inclined wells system (because of the temperature gradient). This means that the horizontal wells system would contain more heat than the inclined wells system.

3.7.4 Injection Temperature

Figure 3.12 (a) represents the temperature decline surface plot obtained by simulating five well models at different injection temperatures, from 80°C to 120°C (other parameters were kept at their medium values). It also indicates that when the water is injected at the minimum temperature (80°C), the temperature of the produced water drops more rapidly than for the maximum injection temperature (100°C). In addition, the temperature of the water produced with 80°C injection is much lower than that with 120°C injection after 30 years. The cumulative amount of heat extracted over 30 years is more for the lower injection temperature (see Figure 3.12 (b)).

The difference in the temperature is the driving factor for heat exchange in a system. The temperature difference also determines the rate of heat transfer from a hot body (rock) to the colder fluid (fluid flowing in the fractures). When cooler water is injected, it extracts more heat from the reservoir and thus drops the temperature of the reservoir more rapidly in a short time. However, warmer injectate helps to maintain a steady decline in reservoir temperature with time. As the total amount of recoverable heat remains constant in this case, the temperature of the injected fluid regulates the rate of heat extraction. Hence the fluid with lower temperature extracts more heat in a 30-year operational period.

3.7.5 Injection Rate

The rate of fluid injection is directly proportional to the rate of heat extraction. A system with high water injection rate will deplete the reservoir faster by extracting more heat and rapidly dropping the temperature in a given time period. However, higher flow rates are not always desirable because there is less residence time within the fracture. With

lower residence time, the water will not be able to extract much heat from the rocks and hence the temperature of produced water would be less. However, as the heat content of any material is the function of the volume and the temperature of the material, the fluid injected at high flow rates having low temperature can still produce more heat compared to low flow rates (see Figure 3.13).

3.7.6 Hierarchy of Factors

Various cases were assessed using surrogate models to determine the hierarchy importance of well spacing, fracture spacing, well inclination angle, injection temperature, and rate of water injected as they affect the temporal heat extraction. One factor was varied at a time while the other four factors were kept constant at their base or central values, i.e., medium values (0). In particular, three outputs are produced from three levels (i.e., low, high, and medium) for the factor of interest while holding other factors at their medium value. Each bar in the tornado plot (Figure 3.14) represents the variation of outputs produced when each variable is set to low (-1), or high (1). The result from medium values (0) of all variables represents the base result and divides the entire range of each variable into two zones. One side depicts the influence of high value of a variable and other side represents the effects of low value.

After repeating the simulations for every factor, bars are arranged from top to bottom according to the total range of output. In other words, the factor that produces the largest variation in results is placed on the top of the chart - representing highest impact. On the other hand, the smallest bar produced by the factor is placed at the bottom. This arrangement of the bar in a single figure takes the appearance of a “tornado”. A tornado

plot for heat extraction after 1 year, 5 years, 15 years, and 30 years is shown in Figure 3.14. A light green bar indicates the impact of the high (1) value, and the brown bar indicates the impact of the low value (-1), on the total heat production. The blue vertical line represents the base value where all factors were taken to have their medium values (0).

Figure 3.14 represents the hierarchy of factors after the end of the first year, fifth year, fifteenth year, and thirtieth year. After one year, the injection flow rate dominates with injection temperature being the second most relevant parameter and spacing is the least relevant. By the end of the first year, there is no interaction among the fractures or among the wells. That is, two consecutive fractures are not competing with each other to extract the heat - similarly for the wells. This indicates that the total amount of heat extracted would mainly be a function of the flow rate and injection temperature. However, as time passes, the fractures and the wells start interacting and compete for heat. The well spacing assumes top priority in terms of recoverable heat. With time, an increase in well spacing would lead to more heat production. Injection temperature, which is inversely proportional to heat extraction, remains the second most relevant parameter. Low injection temperature leads to more rapid heat extraction. Flow rate is the third most important parameter; higher flow rate would produce more heat. Although fracture spacing does not have a high impact after the end of the first year (because there is no interference), after five years it becomes somewhat more important for the cases evaluated. As mentioned previously, well inclination affects the total heat content or the average temperature of the reservoir (a horizontal well has the highest average temperature and a well inclined at 45 degrees has the lowest). For the in-situ properties specified here, it has the least impact on heat production. Figure 3.14 also indicates that all factors do not affect the heat extraction

in the same manner. Well spacing, injection flow rate, and the reciprocal of the well inclination are directly proportional to the amount of heat extracted. Higher values of these three factors would result in higher heat extraction. On the other hand, injection temperature and fracture spacing are inversely proportional to the amount of heat extracted. Low injection temperature and smaller fracture spacing lead to higher heat recovery. The individual impacts of the parameters are summarized in Table 3.4.

3.8 Conclusions

This study considers dominant factors affecting the performance of an EGS and ranks them according to their impact on heat extraction from a reservoir with the properties of the Utah FORGE reservoir. Five important parameters were chosen and their range of values was established by taking data from the Utah FORGE site. The parameters varied in the simulations were grouped into two categories: completion parameters (consisting of well spacing, well inclination, and fracture spacing), and operational parameters (injection temperature and injection flow rate).

Well spacing was identified as the most crucial parameter in terms of the total heat output. Greater well spacing (when possible) also gives the smallest temperature decline over the prescribed 30-year project life. Since well spacing is directly proportional to the total heat output, wells that are widely spaced will extract more heat than closely spaced wells (doublet configuration with one well vertically above and parallel to the other). Injection temperature fell out as the second most important parameter. Since heat production is a function of temperature difference between the reservoir and the circulating fluid, a low temperature injectate will extract more heat than a relatively warmer fluid. The

third most important parameter for the scenario evaluated is the injection flow rate. A greater volume of fluid provides more capacity to extract heat, hence depleting the reservoir faster. Less fracture spacing or more fractures would provide more area for the heat transfer and hence will increase the efficiency of the EGS. The least important parameter for the scenario imagined was the well inclination. A high angle well system (90° to the vertical) would perform better than a low angle well system (45°) because the high angle wells would have slightly higher reservoir temperature.

In order to establish a superior EGS, the first priority is to select a location with excellent natural parameters - high temperature reservoirs at shallow depth. The second priority is to design the well system by carefully considering the impacts of the completion and operational parameters. The natural parameters give the total heat content of the reservoir. By studying the hierarchy of completion parameters, it is possible to design a system to maximize the heat recovery factor. Finally, operational parameters (injection temperature and injection flow rate) can be manipulated to get the appropriate rate of heat extraction from the EGS.

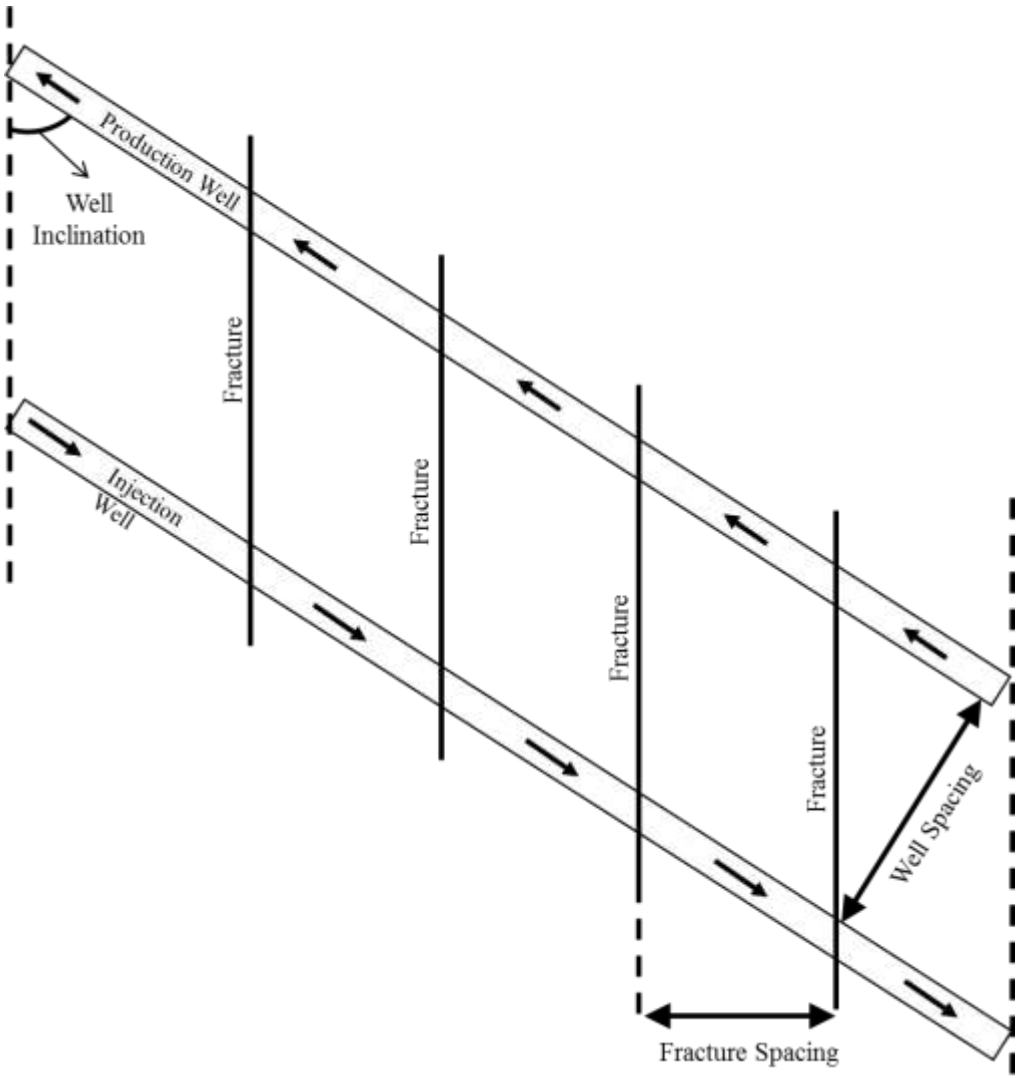

Figure 3.1: Schematic diagram of a doublet EGS with multiple fractures. This is an elevation view.

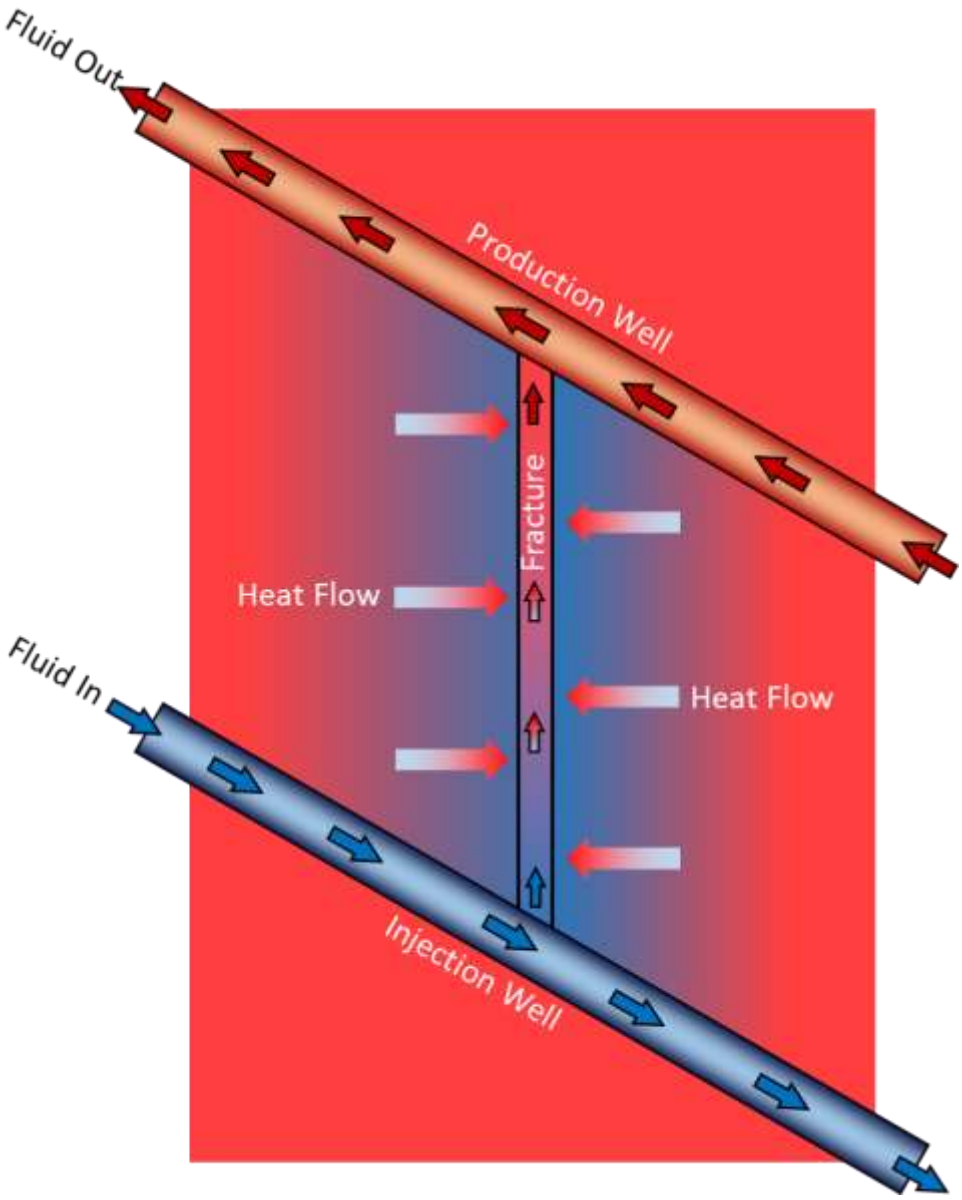

Figure 3.2: Schematic diagram of heat flow in one out of many fractures for a doublet EGS.

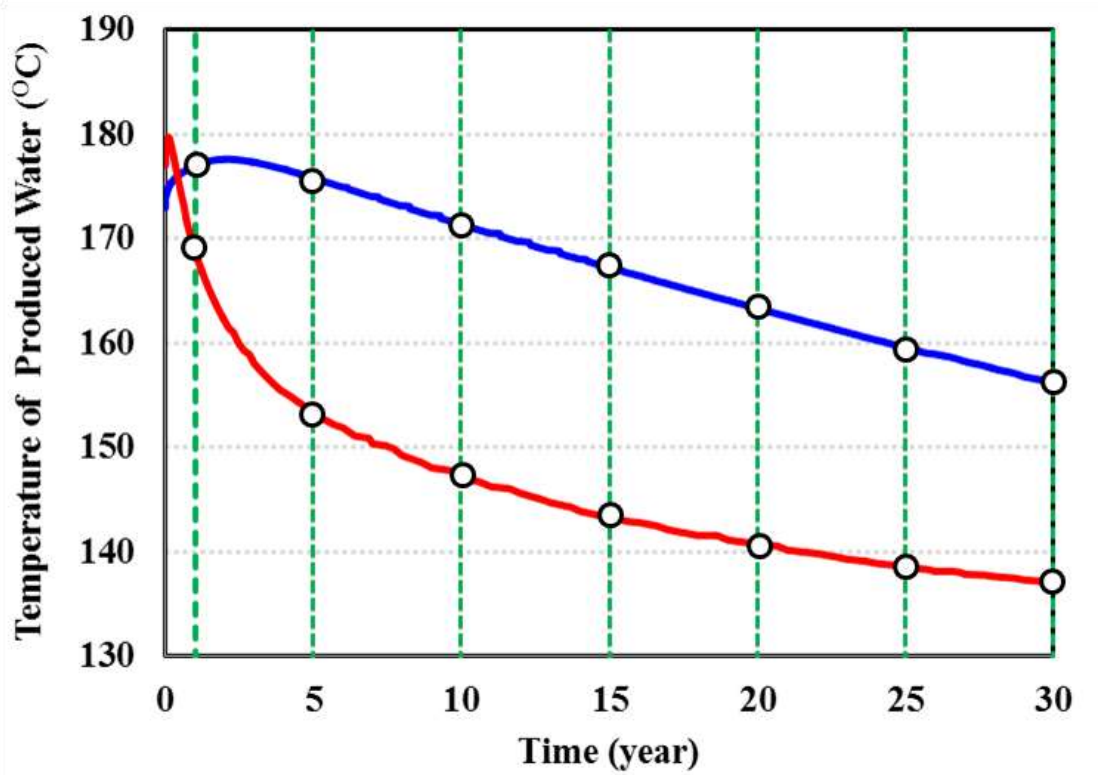

Figure 3.3: Discretization of results of temperature decline curves in time.

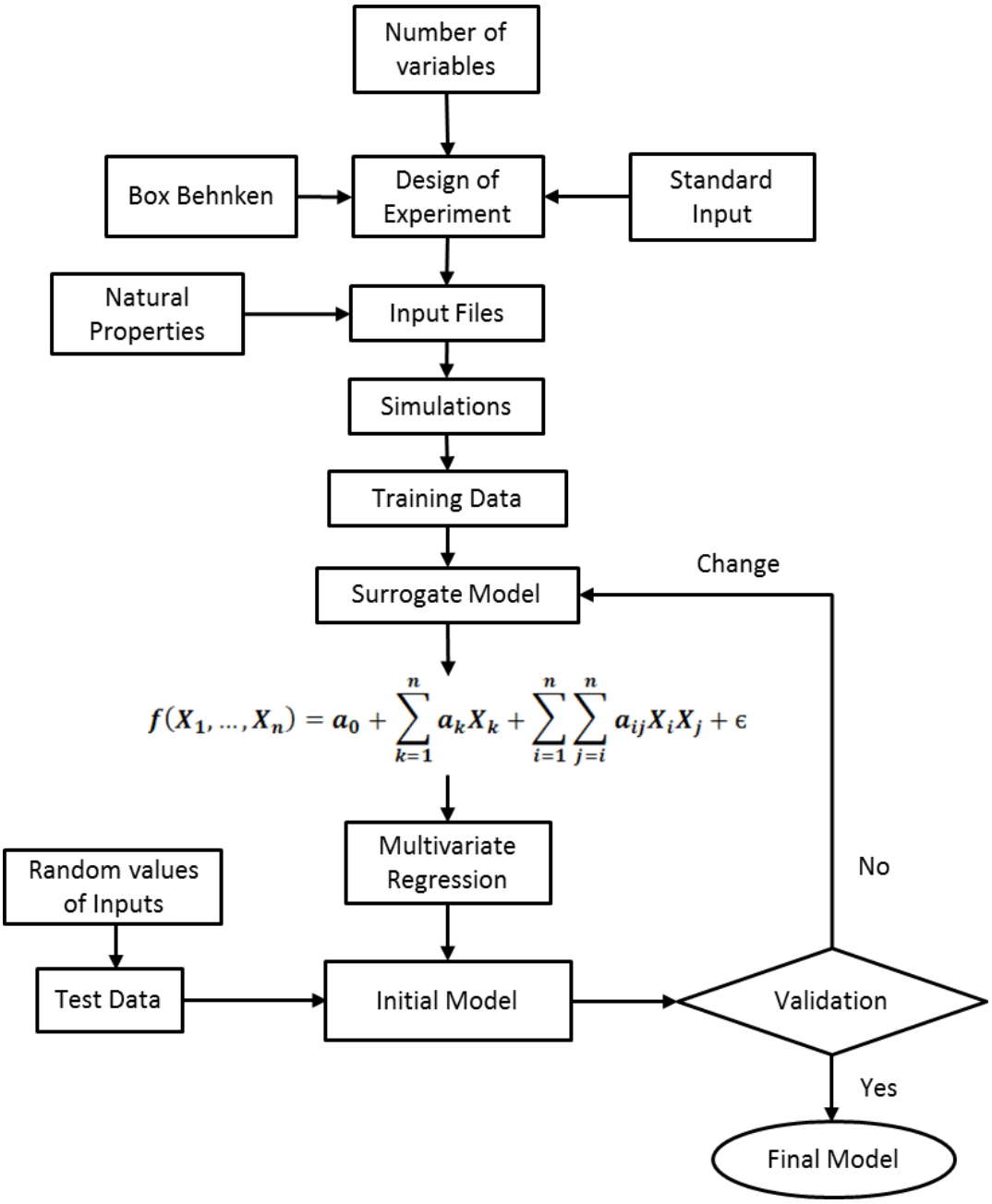

Figure 3.4: Workflow of the methodology to develop a surrogate model.

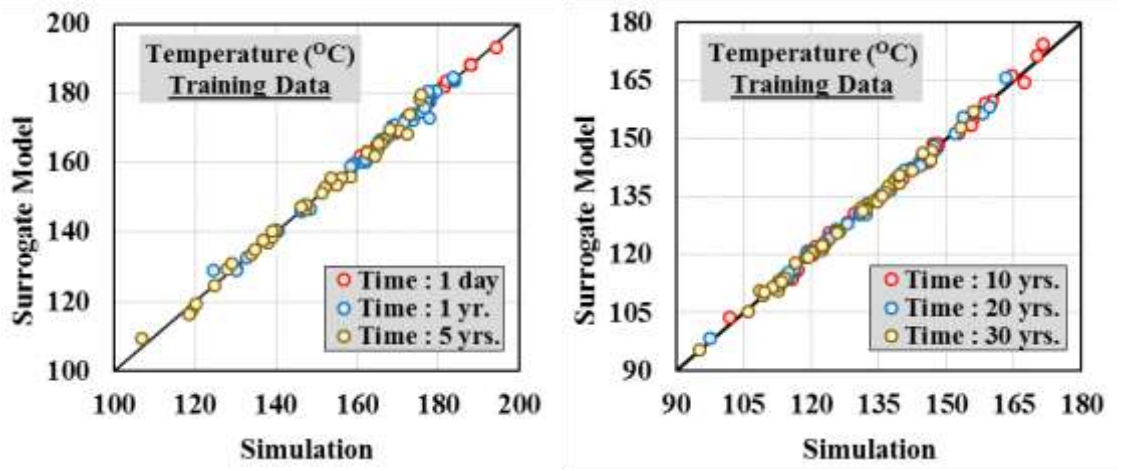

(a) (b)

Figure 3.5: Comparison of training data with the data obtained from the model (a) Data comparison for 1st day, 1st year, and 5th year, (b) Data comparison for 10th year, 20th year and 30th year.

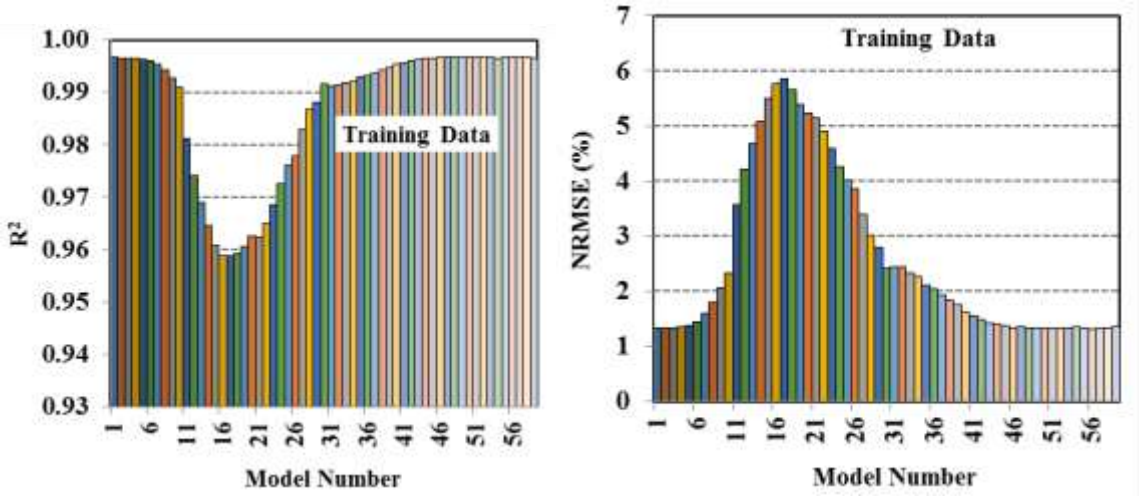

(a) (b)

Figure 3.6: Fitness of RSM model for temperature of produced water for training data (a) Co-efficient of determination, R^2 and (b) NRMSE

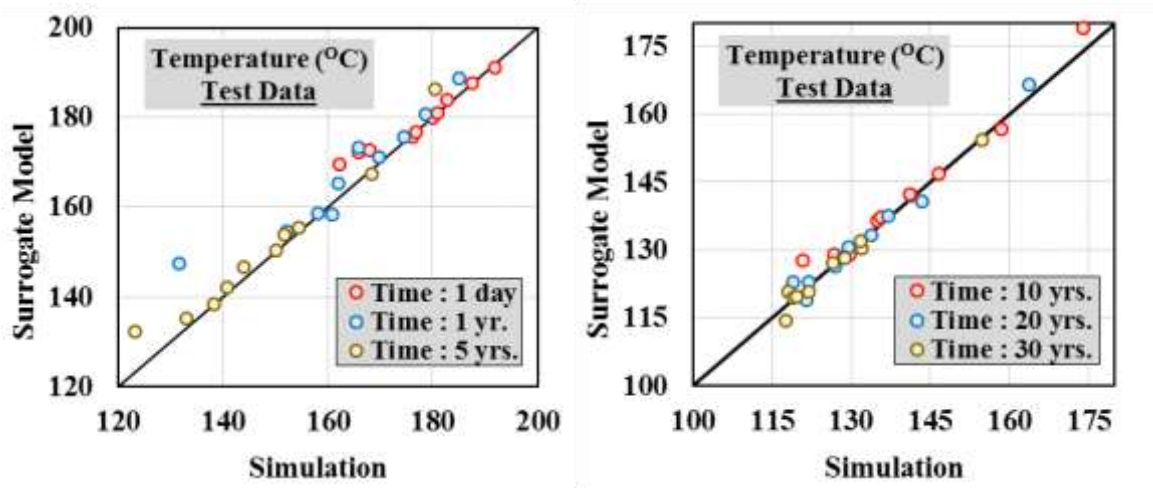

Figure 3.7: Comparison of test data with the data obtained from the model (a) Data comparison for 1st day, 1st year, and 5th year, (b) Data comparison for 10th year, 20th year and 30th year.

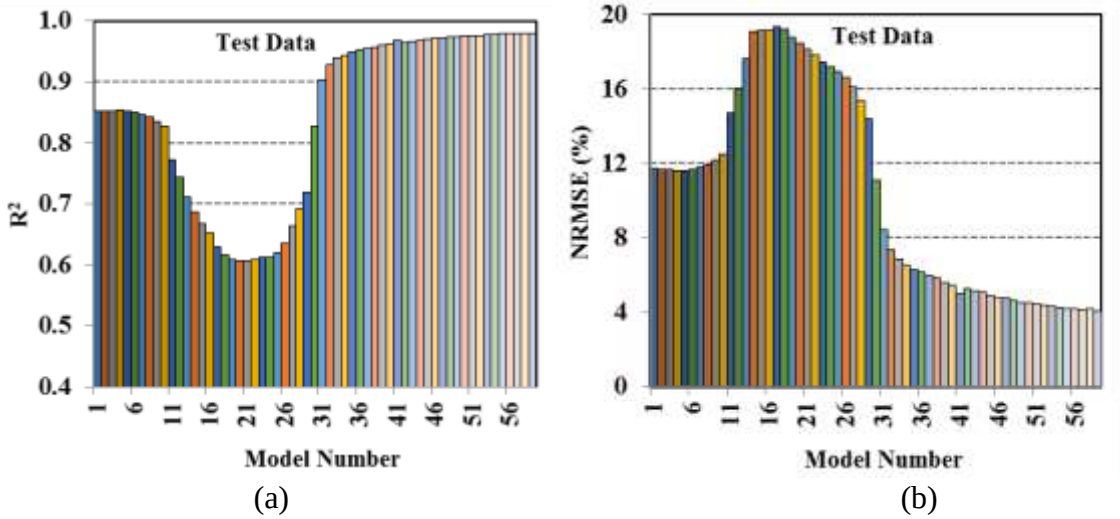

Figure 3.8: Fitness of RSM, ANN, and LSSVM models for temperature of produced water for test data (a) Co-efficient of determination, R^2 and (b) NRMSE.

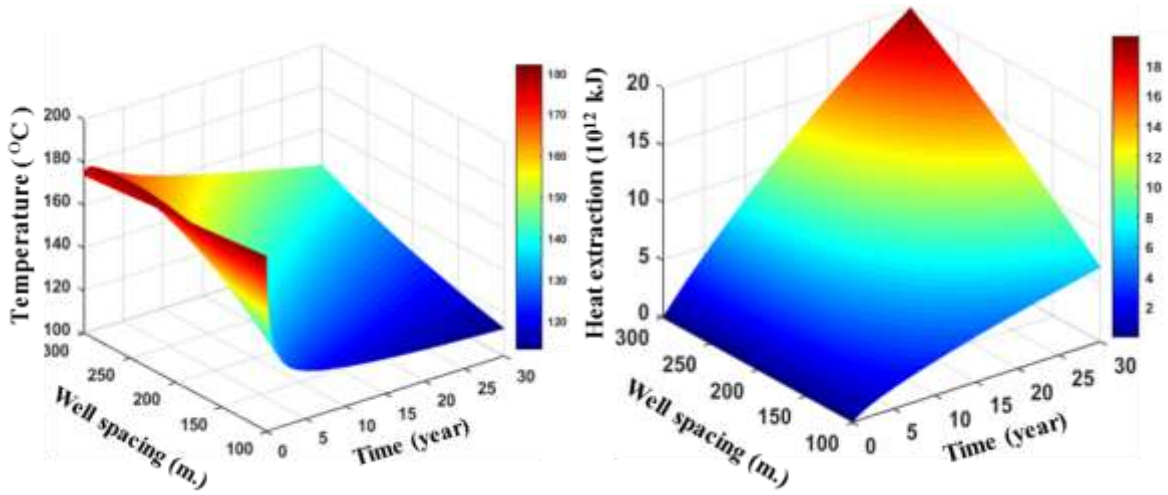

(a) (b)

Figure 3.9: Surface plot of variable well spacing with other parameters at their medium values, (a) Temperature decline in the reservoir (b) Cumulative heat production from the reservoir.

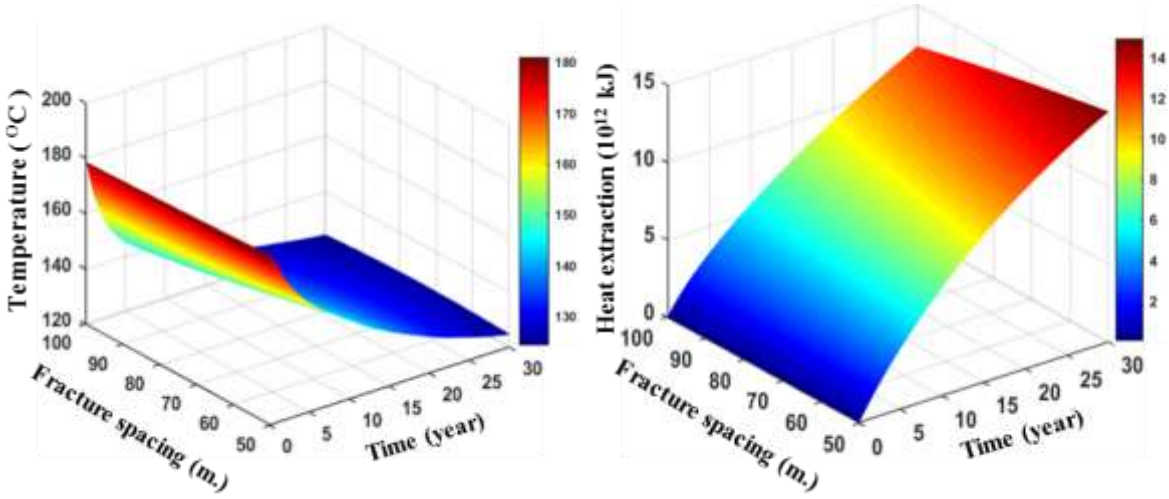

(a) (b)

Figure 3.10: Surface plot of variable fracture spacing with other parameters at their medium values, (a) Temperature decline in the reservoir (b) Cumulative heat production from the reservoir.

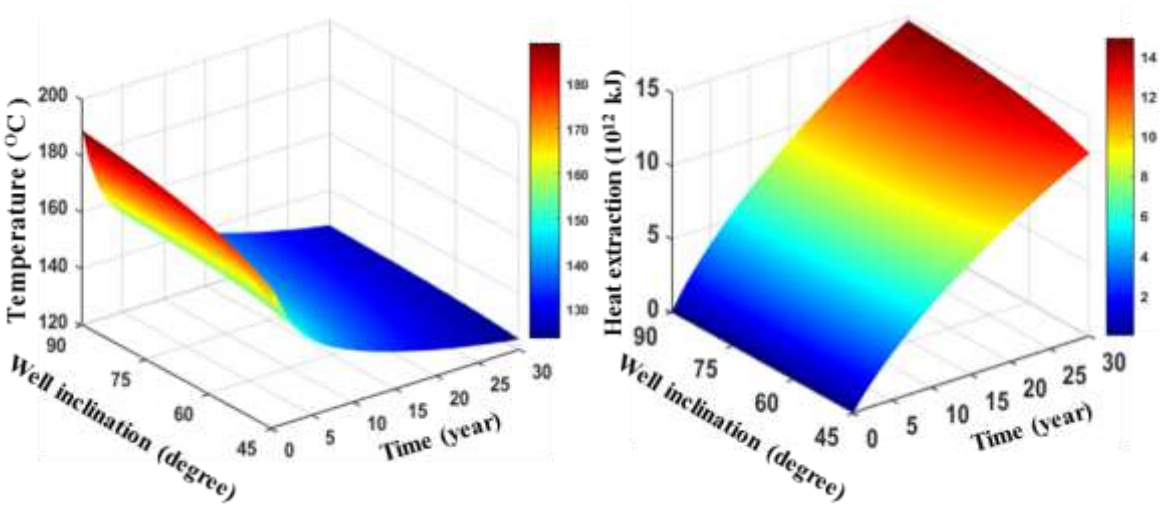

(a) (b)

Figure 3.11: Surface plot of variable angle of well inclination with other parameters at their medium values, (a) Temperature decline in the reservoir (b) Cumulative heat production from the reservoir.

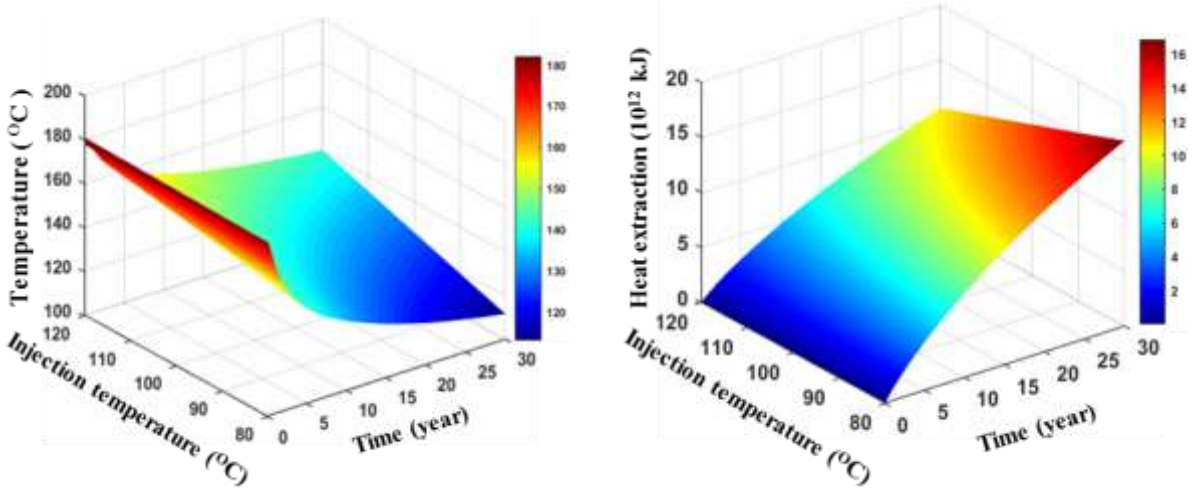

(a) (b)

Figure 3.12: Surface plot of variable injection temperature with other parameters at their medium values, (a) Temperature decline in the reservoir (b) Cumulative heat production from the reservoir.

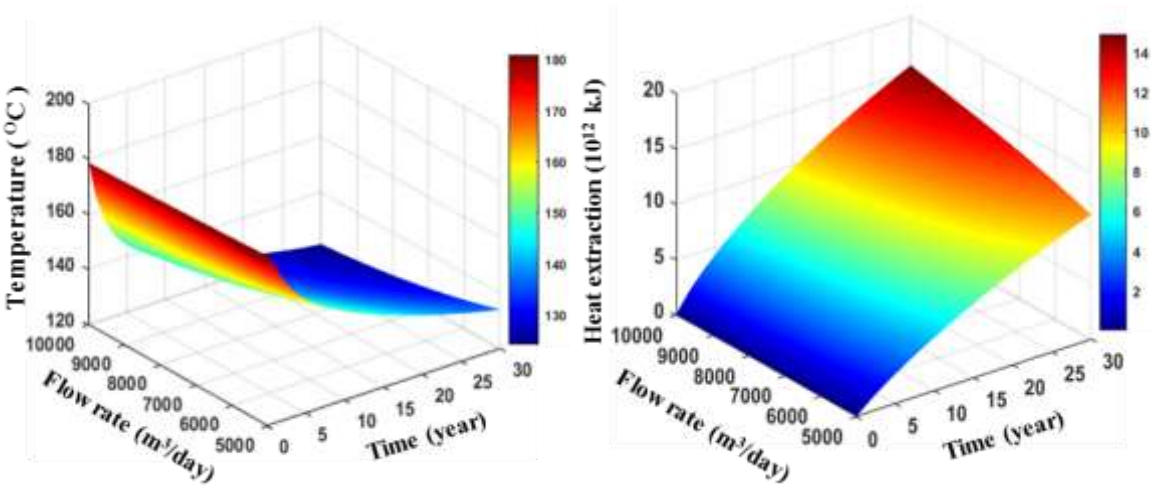

(a) (b)

Figure 3.13: Surface plot of variable flow rate with other parameters at their medium values, (a) Temperature decline in the reservoir (b) Cumulative heat production from the reservoir.

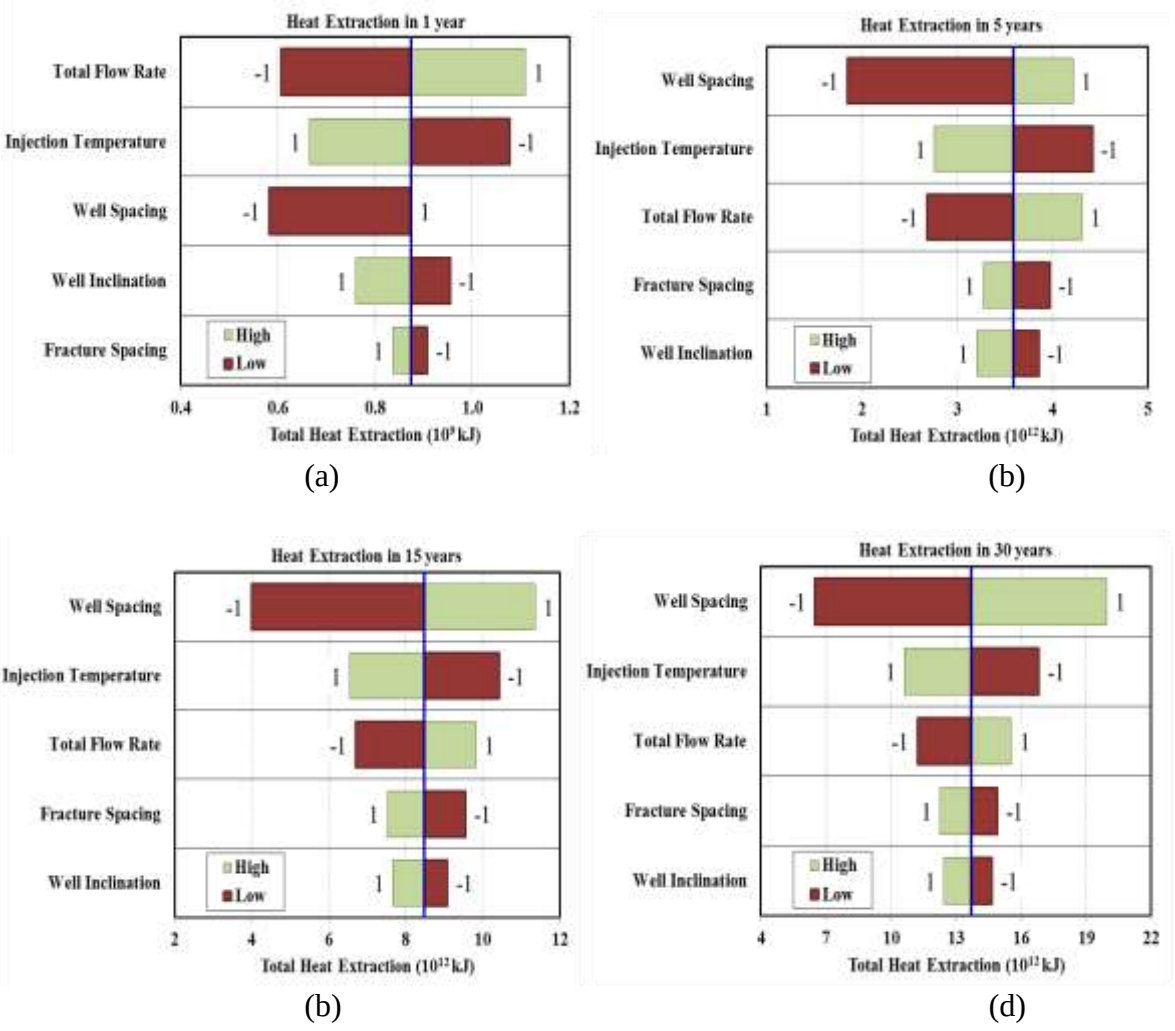

Figure 3.14: Hierarchy of all the parameters with time, (a) At the end of the first year, (b) At the end of five years, (c) At the end of 15 years, (d) At the end of 30 years.

Table 3.1: Dimension of entire reservoir model

Dimensions	Entire Reservoir
Reservoir length (X-direction), m	900
Reservoir width (Y-direction), m	500
Reservoir height (Z-direction), m	Depends on well inclination and well spacing
Fracture width, m	0.01
Fracture height, m	200-600 (Depends on well inclination and well spacing)

Table 3.2: Natural properties of the FORGE site

Properties	Value
Density of the rock, (kg/m^3)	2700
Permeability of the formation, (mD)	0.01
Permeability of the fractured zone, (mD)	50000
Porosity of the formation	0.01
Porosity of the fractured zone, (%)	10
Water Saturation, (%)	100
Thermal conductivity of formation, $(J/(m.day.℃))$	$2.592 \text{ X } 10^5$
Thermal conductivity of water, $(J/(m.day.℃))$	$5.18 \text{ X } 10^4$
Volumetric heat capacity of the formation, $(J/(m^3.℃))$	$2.133 \text{ X } 10^6$
Specific heat capacity of the fluid , $(J/(m^3.℃))$	4818
Formation compressibility, $(1/kPa)$	$4.4 \text{ X } 10^{-7}$
Temperature gradient, $(℃/m)$	0.06
Reference depth, (m)	2520
Reference temperature, $(℃)$	200

Table 3.3: Input parameters

	Variable	Symbol	Minimum (-1)	Medium (0)	Maximum (+1)
1	Well spacing, (meter)	X1	100	200	300
2	Fracture spacing, (meter)	X2	50	75	100
3	Angle of well inclination, (1/degree)	X3	1/90	1/60	1/45
4	Injection temperature (^{O}C)	X4	80	100	120
5	Total injection rate (m^3/day)	X5	5000	7500	10000

Table 3.4: Parameter ranks, relation with heat extraction, and their physical effects on EGS over 30 years

Impact Rank	Parameter	Relation with Heat output	Physical Impacts
1	Well spacing	Direct	Affects the primary heat recovery factor for the EGS.
2	Injection temperature	Inverse	Affects the rate of heat extraction for the EGS
3	Total injection rate	Direct	Affects the rate of heat extraction for the EGS
4	Fracture spacing	Inverse	Affects the secondary heat recovery factor
5	Angle of well inclination	Direct	Affects the average temperature of the volume “enclosed” by the two well system.

3.9 Appendix

All variables except well inclination are transformed from their actual values to encompass a range from -1 to +1 as follows.

$$\text{Transformed variable,} \qquad X = 2\frac{\text{Actual value} - \text{Low}}{\text{High} - \text{Low}} - 1 \qquad (3.3)$$

Well inclination angle is transformed as follows

$$\text{Transformed variable,} \qquad X = 2\frac{\frac{1}{\text{Actual value}} - \frac{1}{\text{Low}}}{\frac{1}{\text{High}} - \frac{1}{\text{Low}}} - 1 \qquad (3.4)$$

Table 3.5: Values of inputs for simulations of training data

Simulation No.	Input Factors				
	Well spacing	Fracture Spacing	Well inclination	Injection temperature	Injection rate
1	-1	-1	0	0	0
2	-1	1	0	0	0
3	-1	0	1	0	0
4	-1	0	-1	0	0
5	-1	0	0	-1	0
6	-1	0	0	1	0
7	-1	0	0	0	-1
8	-1	0	0	0	1
9	0	0	1	-1	0
10	0	0	1	1	0
11	0	0	-1	-1	0
12	0	0	-1	1	0
13	0	-1	0	0	-1
14	0	-1	0	0	1
15	0	1	0	0	-1
16	0	1	0	0	1
17	0	0	0	-1	-1
18	0	0	0	-1	1
19	0	0	0	1	-1
20	0	0	0	1	1
21	0	-1	1	0	0
22	0	-1	-1	0	0
23	0	1	1	0	0
24	0	1	-1	0	0
25	0	0	1	0	-1
26	0	0	1	0	1
27	0	0	-1	0	-1
28	0	0	-1	0	1
29	0	-1	0	-1	0
30	0	-1	0	1	0
31	0	1	0	-1	0
32	0	1	0	1	0
33	0	0	0	0	0
34	1	-1	0	0	0
35	1	1	0	0	0
36	1	0	1	0	0
37	1	0	-1	0	0
38	1	0	0	-1	0

Table 3.5: (continued)

Simulation No.	Input Factors				
	Well spacing	Fracture Spacing	Well inclination	Injection temperature	Injection rate
39	1	0	0	1	0
40	1	0	0	0	-1
41	1	0	0	0	1

Table 3.6: Values of inputs for simulations of test data

Simulation No.	Input Factors				
	Well spacing	Fracture Spacing	Well inclination	Injection temperature	Injection rate
1	-0.500	0.200	0.000	0.533	0.138
2	0.500	-0.800	0.000	-0.199	0.122
3	-0.800	-0.200	0.000	0.377	0.420
4	-0.150	-0.600	0.500	0.102	0.598
5	0.900	-0.400	-1.000	-0.195	-0.847
6	0.300	0.600	0.000	0.168	0.634
7	0.100	0.200	-1.000	0.424	0.533
8	-0.250	0.800	0.500	0.041	0.435
9	0.600	-0.200	0.500	-0.769	0.683
10	-0.600	-0.800	-1.000	-0.002	0.748

Table 3.7: Error analysis of various models

Model No.	Model (day)	R^2		NRMSE	
		Training	Test	Training	Test
1	1	0.997	0.852	1.3	11.8
2	2	0.997	0.852	1.3	11.7
3	3	0.997	0.853	1.3	11.6
4	4	0.996	0.853	1.4	11.6
5	5	0.996	0.852	1.4	11.6
6	6	0.996	0.850	1.4	11.6
7	7	0.995	0.847	1.6	11.8
8	8	0.994	0.842	1.8	11.9
9	9	0.993	0.836	2.1	12.2
10	10	0.991	0.828	2.3	12.5
11	15	0.981	0.773	3.6	14.7
12	18	0.974	0.744	4.2	16.0
13	21	0.969	0.711	4.7	17.6
14	24	0.965	0.687	5.1	19.1
15	27	0.961	0.668	5.5	19.1
16	30	0.959	0.653	5.8	19.1
17	35	0.959	0.630	5.9	19.3
18	40	0.959	0.616	5.7	19.2
19	45	0.960	0.609	5.4	18.8
20	50	0.963	0.606	5.2	18.4
21	55	0.962	0.607	5.1	18.1
22	60	0.965	0.609	4.9	17.8
23	70	0.969	0.612	4.6	17.4
24	80	0.973	0.612	4.3	17.2
25	90	0.976	0.621	4.0	16.9
26	100	0.978	0.636	3.9	16.6
27	120	0.983	0.663	3.4	16.1
28	150	0.987	0.692	3.0	15.3
29	181	0.988	0.720	2.8	14.4
30	365	0.992	0.828	2.4	11.1
31	730	0.991	0.903	2.4	8.4
32	1095	0.991	0.928	2.4	7.4
33	1461	0.992	0.939	2.3	6.8
34	1826	0.992	0.944	2.3	6.6
35	2191	0.993	0.949	2.1	6.3
36	2556	0.993	0.952	2.0	6.1
37	2922	0.994	0.955	1.9	5.9
38	3287	0.994	0.957	1.8	5.8

Table 3.7: (continued)

Model No.	Model (day)	R^2		NRMSE	
		Training	Test	Training	Test
39	3652	0.995	0.961	1.8	5.6
40	4017	0.995	0.962	1.6	5.4
41	4383	0.996	0.968	1.6	5.0
42	4748	0.996	0.965	1.5	5.2
43	5113	0.996	0.966	1.4	5.2
44	5478	0.996	0.967	1.4	5.1
45	5844	0.997	0.969	1.4	4.9
46	6209	0.997	0.971	1.3	4.8
47	6574	0.997	0.972	1.3	4.7
48	6939	0.997	0.973	1.3	4.6
49	7305	0.997	0.974	1.3	4.5
50	7670	0.997	0.975	1.3	4.5
51	8035	0.997	0.975	1.3	4.4
52	8400	0.997	0.976	1.3	4.4
53	8766	0.997	0.977	1.3	4.3
54	9131	0.996	0.978	1.4	4.2
55	9496	0.997	0.979	1.3	4.2
56	9861	0.997	0.979	1.3	4.2
57	10227	0.997	0.979	1.3	4.1
58	10592	0.997	0.979	1.3	4.2
59	10957	0.997	0.980	1.3	4.1

3.10 References

[1] M.C. Smith, R.L. Aamodt, R.M. Potter, and D.W. Brown, Manmade Geothermal Reservoirs, LA-UR-75-953.CONF-750525-6. 1975, Los Alamos Scientific Laboratory, : New Mexico, USA.

[2] A.S. Batchelor, The creation of Hot Dry Rock systems by combined explosive and hydraulic fracturing. in International conference on geothermal energy. (1982).

[3] F.H. Cornet, Experimental investigations of forced fluid flow through a granite rock mass in Proceedings of 4th International Seminar on the Results of EC Geothermal Energy Demonstration, April 27-30. Florence, Italy (1989).

[4] (DOE), D.o.E., An Evaluation of Enhanced Geothermal Systems Technology:Geothermal Technologies Program. 2008.

[5] S.K. Sanyal, and S.J. Butler. An analysis of power generation prospects from enhanced geothermal system. in Proceedings World Geothermal Congress, 24-29 April. Antalya, Turkey (2005).

[6] L.P. Frash, M. Gutierrez, J. Hampton, and J. Hood, Laboratory simulation of binary and triple well EGS in large granite blocks using AE events for drilling guidance. Geothermics, 55 (2015). p. 1-15.

[7] Z. Sun, X. Zhang, Y. Xu, J. Yao, H. Wang, S. Lv, Z. Sun, Y. Huang, M. Cai, and X. Huang, Numerical simulation of the heat extraction in EGS with thermal-hydraulic-mechanical coupling method based on discrete fractures model. Energy, 120 (2017). p. 20-33.

[8] Y. Xia, M. Plummer, E. Mattson, R. Podgorney, and A. Ghassemi, Design, modeling, and evaluation of a doublet heat extraction model in enhanced geothermal systems. Renewable Energy, 105 (2017). p. 232-247.

[9] M.D. Aliyu, and H.P. Chen, Optimum control parameters and long-term productivity of geothermal reservoirs using coupled thermo-hydraulic process modelling. Renewable Energy, 112 (2017). p. 151-165.

[10] P. Panja, M. Pathak, R. Velasco, and M. Deo. Least Square Support Vector Machine: An Emerging Tool for Data Analysis. in SPE Low Perm Symposium, 5-6 May. Colorado, Denver: Society of Petroleum Engineers (2016).

CHAPTER 4

FLUID FLOW DISTRIBUTION IN FRACTURES FOR A DOUBLET SYSTEM IN ENHANCED GEOTHERMAL SYSTEMS (EGS)[3]

4.1 Abstract

Extraction of heat from an enhanced geothermal system (EGS) is a renewable and environmentally benign technology. The process involves circulation of colder water in hot rock through a flow path consisting of an injection well, several vertical fractures, and a production well. In this process, distribution of water among the vertical fractures is one of the key factors for optimization of heat recovery. Geometry, dimensions or total flow area, and fluid velocity in wells and fractures play a major role in the hydrodynamics in the loop. A mathematical model is developed from the analogy of an electrical circuit applying Kirchhoff's law to determine the pressure drop between two points. Accordingly, the flow rates through fractures are calculated. Maintenance of sufficient pressure in a fracture is necessary to avoid closure due to horizontal stress. In this model, variation of fracture width with pressure is considered. The impacts of injection rate, well diameter, and number of fractures on the distribution of flow in fractures are also investigated in this study. Since the frictional loss along the well decreases with the increase in well diameter,

3 Pranay Asai, University of Utah; Palash Panja, University of Utah; John McLennan, University of Utah; Joseph Moore, University of Utah

fewer variations of flow rates in fractures are observed. Similarly, low fluid velocity due to low total flow rate causes less frictional loss, thus more even distributions of flow in the fracture are seen. The number of fractures completed in an EGS is an important parameter for optimization. The flow distribution among the fractures depends on the total number of fractures present in the system. Although more fractures improve the heat recovery, the cost of completion increases with the number of fracture. The analytical model for flow distribution developed in this study is helpful to evaluate the effectiveness of an EGS and to optimize the completion and operational parameters.

4.2 Keywords

Enhanced Geothermal System (EGS); Heat recovery in EGS; Flow distribution in EGS; Multifractured EGS; Fracture width with pressure

4.3 Introduction

For more than a century, geothermal energy has been exploited to produce electricity and provide direct heating. The key to avail this huge resource lies in understanding the geothermal reservoir. Parameters such as the temperature of the reservoir, depth, reservoir size, heat capacity, and permeability are a few of the properties that need to be evaluated and studied. This is in addition to the availability of a working fluid. In the absence of mobile water, one way to tap into this huge heat source is by developing an enhanced geothermal system (EGS) [1, 2]. An EGS consists of sets of wells, drilled a few hundred meters apart. These wells are interconnected by creating multiple hydraulic fractures. Then, a working fluid (which helps in transporting the heat to the

surface) is injected into one or multiple wells, passing through the fractures and brought back to the surface via production wells. While this fluid passes through the fractures, it takes on heat from the formation and brings it out to the surface where it is flashed to steam or run through an organic Rankine cycle heat exchange system. An EGS can consist of any number of wells and multiple stages of hydraulically-induced fractures.

This study assesses the thermo-hydraulic flow distribution within these hydraulic fractures, in a horizontal doublet system. A doublet system consists of an injection well and a production well. There would be multiple fractures along the length of the injection well, and these are explicitly connected to the production well. When the working fluid is pumped into the injection well, it is distributed into the fractures and produced via the production well. As the fluid passes through the fractures, it acquires heat from the reservoir. If more fluid is pumped, it would extract more heat, although the thermal resource is fundamentally finite in the longer term. To ensure that heat is withdrawn uniformly along the length of the wellbore doublet, it is important to comprehend the flow distribution among the fractures.

There have been many studies to understand the flow patterns in a single fracture geothermal system. Zeng et al. [3] evaluated the performance of a horizontal doublet system, and concluded that the key factors affecting the energy efficiency are permeability and the water flow rate. Guo et al. [4] studied the thermal drawdown in a single fracture and evaluated the flow patterns in the fracture and their effect on heat production. Al-Rbeawi [5] analyzed the behavior of flow regimes in natural and hydraulically-induced fractured unconventional gas reservoirs and studied the pressure behavior.

Other studies that were carried out on multifractured EGS had a basic assumption

that all the fractures take the same amount of fluid. Zeng et al. [6] estimated the parameters that affect the power efficiency and life of the EGS by studying the flow in a doublet multifractured system. Li et al. [7] performed thermal breakdown calculations to optimize the multistage EGS by assuming equal flow rates in all the fractures. Wu et al. [8] studied the heat extraction in a vertical doublet system with multiple fractures and also assumed equal flow rates in all the stages. Xia el al. [9] evaluated the design and modeling of a doublet EGS with equal flow rates in all the fractures. As there has been negligible research related to analyzing the flow distribution in a multifractured enhanced geothermal system, it is important to validate the assumption of equal distribution of fluid.

This study focuses on creating an analytical model to study the flow distribution among the fractures in an EGS. The mathematical model is derived as an analog to the principle of Kirchhoff's law for current distribution in a closed multiloop circuit. The resistance to the fluid flow in the pipe and inside the fractures would be used as the criteria to distribute the fluid among the fractures.

4.4 Representation of an EGS Doublet System

The EGS system used to carry out this study includes a doublet well system consisting of two horizontal wells at the same depth and some appropriate distance apart. The wells have multiple fracture stages, along their lengths (see Figure 4.1).

As shown in Figure 4.1, there are two wells (injection and production wells), and 'n' fractures. The fracture numbering starts from the toe of the wells (end of the wells). 'F_n' represents the fracture number, 'w_n' represents the average width of the nth fracture, 'P_{inj}^n' represents the injection pressure at the entrance of the nth fracture, 'P_{out}^n' represents

the outlet pressure at the nth fracture. 'X_F' represents the fracture spacing and 'X_L' represents the spacing between the two wells.

Each fracture provides a pathway for the fluid to move through the nominally impermeable reservoir and connects the wells. This facilitates the circulation of fluid through the reservoir. The fractures are taken to propagate in the direction of the maximum principal stress. In reality, this propagation is further affected by the presence of natural fractures, thus making it very complex in nature. To perform the calculations and keep the model simple, the fractures were considered to be circular (penny shaped in the jargon of hydraulic fracturing and fracture mechanics). The center of this circular facture lies between the two wells and the fracture has a concave shape. Each circular fracture has a diameter equal to the well spacing, and its width varies with the distance from the center. Again, to maintain simplicity in the calculations, an average width was calculated and the fracture was considered to be planar (as shown in Figure 4.2).

4.5 Analogy to Kirchhoff's Voltage law

According to the Kirchhoff's law used for closed electric circuits, division of the current within the loop takes place according to the resistance present in the circuit. That means, more current would flow where the resistance is the least. The current flowing through a resistance would determine the potential difference across it. Consequently, in a multiloop system having multiple resistances of the same value, each branch would carry an equal amount of current (Figure 4.3) and would have the same amount of potential difference across it.

However, when the resistances in the loops are different from each other, the

current distribution is governed by Kirchhoff's law. Each branch carries a different amount of current and hence would have a different potential across it (see Figure 4.4).

Similarly, when the fluid flows through fractures in a fractured geothermal doublet, it tends to take the path of least resistance. The distribution would depend on the factors causing the resistance to the flow. In a closed loop system with two wells and multiple fractures, the resistance is mainly caused by the frictional force acting opposing the direction of the flow. The fluid flowing in the system is analogous to the current flowing in an electric circuit. The frictional resistance in the fracture and in the injection and production well tubulars is analogous to the resistance in the circuit and the pressure is analogous to the potential difference across the resistance. Neglecting the frictional losses within the wellbore, there would be an equal distribution of fluid in each fracture.

Analogous to the resistance in the electric circuit, the frictional resistance in the well system is dependent on the flow rate. That means the frictional losses would depend on the flow rate in the particular section and thus would change the flow distribution within the fracture. Additional complexities can arise if the flow is turbulent as opposed to laminar (i.e., a non-first order dependence of friction pressure loss on the volumetric flow rate). Hence, it is necessary to iterate the equations until convergence of the rate and pressure in each fracture is achieved.

4.5.1 Mathematical Representation

To determine the flow distribution among multiple fractures, a simple case consisting of two fractures is considered first. Figure 4.5 represents a system consisting of two parallel wells separated horizontally by a distance $\boldsymbol{X_L}$, with two fractures a distance $\boldsymbol{X_F}$

apart. The fractures are numbered starting from the last fracture at the end of the wells (toe of the well). Fluid would be injected into the injection well at a rate of Q and at an injection pressure of P_{in}. When the system reaches steady state, the flow rate into the first and second fractures is given as q_1 and q_2, respectively. Fracture one and fracture two will have widths w_1 and w_2, respectively. Since the fractures are circular, it is assumed that the fluid distributes instantaneously over the fracture area and the maximum area of the cross-section in the fracture is taken as the average area of cross-section for the fluid flow across the fracture[4]. The flow across the fracture will cause a drop in the injection pressure due to the friction inside the fracture. In a general situation, for the n^{th} fracture, the frictional pressure drop, $'\Delta P_{frac,\ n}'$, caused by a fluid with a density, $'\rho'$, flowing at a rate, $'q_n'$, inside a fracture whose length is $'X_l'$, with a hydraulic diameter, $'d_h'$, and a cross-sectional area, $'A_f'$, is given by Equation 4.1, where the $'f_{f_{q_n}}'$ represents the Fanning friction factor. The coefficient of friction varies with the type of flow inside the fracture and can be estimated accordingly.

$$\Delta P_{frac,\ n} = f_{f_{q_n}} \frac{2X_l}{d_h} \rho \left(\frac{q_n}{A_f}\right)^2 \qquad (4.1)$$

Similarly, there is another frictional pressure drop as the fluid passes through the pipe sections between two consecutive fractures. For the section between the n^{th} and $(n-1)^{th}$ fracture, which are $'X_f'$ distance apart, the frictional pressure drop, $'\Delta P_{pipe,\ n}'$, caused by a fluid with a density, $'\rho'$, flowing at a rate, $'q_{p,n}'$, inside a pipe with a hydraulic diameter, $'D_h'$, and a cross-sectional area, $'A_p'$, is given by Equation 4.2, where $'f_{p_{q_n}}'$ represents the Fanning friction factor for flow in a circular pipe. The coefficient of friction

4 The approximations built into this simplification are acknowledged.

varies depending on the type of flow inside the pipe (laminar, transitional, or turbulent) and can be estimated accordingly. Entrance and exit losses and minor losses associated with valves or other components are not considered but could be easily added.

$$\Delta P_{pipe,\ n} = f_{p_{q_n}} \frac{2X_f}{D_h} \rho \left(\frac{q_{p,n}}{A_p} \right)^2 \qquad (4.2)$$

Considering the two inlets and two outlets for the fractures as nodal points, Kirchhoff's law for current allocation can be applied to the system. In this case, the pressure is analogous to the potential difference, flow rate is analogous to the current, and the friction in the pipe and the fractures are analogous to the resistance. The outlet pressure for the second fracture, $'P_{out}^2'$, can be calculated directly by subtracting the pressure drop across the second fracture (see Equation 4.3) and also by traversing through the pipe section, the first fracture and another pipe section (see Equation 4.4).

$$P_{out}^2 = P_{in}^2 - f_{F_{q2}} \frac{2x_L}{d_h} \rho \left(\frac{q_2}{A_f} \right)^2 \qquad (4.3)$$

$$P_{out}^2 = P_{in}^2 - 2f_{p_{q1}} \frac{2x_f}{D_h} \rho \left(\frac{Q - q_2}{A_P} \right)^2 - f_{F_{q1}} \frac{2x_L}{d_h} \rho \left(\frac{q_1}{A_f} \right)^2 \qquad (4.4)$$

Since there are many constants in Equation 4.4, some of these constants can be grouped together as shown in the Equation 4.5 and 4.6 (this is done for convenience and these are dimensional constants). When Equations 4.3 and 4.4 are equated and Equation 4.5 and Equation 4.6 are substituted into that relationship, the flow rate in the individual fractures is represented by Equation 4.7 and 4.8.

$$f_{P_{qn}} \frac{2\rho x_f}{D_h {A_P}^2} = b_{P_{qn}} \qquad (4.5)$$

$$f_{F_{qn}} \frac{2\rho x_L}{d_h {A_f}^2} = b_{F_{qn}} \qquad (4.6)$$

$$q_2 = Q\frac{\left(\frac{2b_{P_{q1}} + b_{F_{q1}}}{b_{F_{q2}}}\right)^{\frac{1}{2}}}{\left(\frac{2b_{P_{q1}} + b_{F_{q1}}}{b_{F_{q2}}}\right)^{\frac{1}{2}} + 1} \qquad (4.7)$$

$$q_1 = Q\frac{1}{\left(\frac{2b_{P_{q1}} + b_{F_{q1}}}{b_{F_{q2}}}\right)^{\frac{1}{2}} + 1} \qquad (4.8)$$

These equations can be generalized for a system consisting of $'N'$ fractures as shown in Figure 4.6. The flow through the n^{th} fracture can be estimated by Equations 4.9 and 4.10. Derivations of these generalized equations are summarized in Appendix 4.9

$$c_n = \frac{\left(\frac{2b_{P_{q(n-1)}} + b_{F_{q(n-1)}}\left(c_{(n-1)}\right)^2}{b_{F_{qn}}}\right)^{\frac{1}{2}}}{\left(\frac{2b_{P_{q(n-1)}} + b_{F_{q(n-1)}}\left(c_{(n-1)}\right)^2}{b_{F_{qn}}}\right)^{\frac{1}{2}} + 1} \qquad (4.9)$$

$$q_n = \left(Q - \left(\sum_{i=n}^{N} q_{n+1}\right)\right)c_n \qquad (4.10)$$

All the frictional resistances for the n^{th} fracture (resistance in the fracture and the pipe sections) can be grouped together and rewritten as a simplified constant $'c_n'$, to calculate the flow in the $'n^{th}'$ fracture, with the $'c_1 = 1'$.

Since the constants $b_{P_{qn}}$ and $b_{F_{qn}}$ are functions of the flow rate, it is not possible to write the equations in an explicit form. Multiple iterations need to be carried out by assuming the initial flow distribution in the system and solved until convergence is achieved.

It is important to choose the initial flow distribution carefully because this governs the initial pressure distribution in the system. The inlet pressure at the nearest fracture (the one at the heel of the wells) is the nodal point for the highest pressure and the outlet pressure at the last fracture is the nodal point for the lowest pressure in the system to ensure the flow inside the fracture system. Since the width of the fracture depends on the injection and outlet pressures across the fracture and a higher flow rate would cause greater pressure drop, the last fracture (the one at the heel of the wells) will have the highest flow rate. As a result, while choosing the initial distribution, if higher flow rates are chosen for the fractures at the toe of the well, this might give negative pressure values and will preclude accurate results. Hence, it is important to divide the initial flow in such a way that the first fracture at the toe of the well gets the minimum amount of fluid so as to reduce the frictional losses in the pipe and within the first fracture at the toe of the well.

One of the way to estimate the initial flow distribution is by dividing the flow using a high degree polynomial distribution. This will ensure that the first fracture (at the toe) takes the least amount of fluid and the last fracture (at the heel) takes the largest amount. The polynomial distribution of the total flow rate, $'Q'$, for the n^{th} fracture in a system consisting of N fractures is shown in Equation 4.11.

$$q_n = \frac{n^x}{\sum_{i=1}^{N} i^x} Q \qquad (4.11)$$

4.5.2 Equation Validation

Rudimentary equations have been derived for the flow distribution at steady state in a doublet well system. In order to qualitatively check their validity, the relationships were tested with several injection scenarios and the results were analyzed.

The first validation method is to assume that there are no frictional losses in any of the tubulars. This means that the pressure loss term due to pipe friction is zero. This indicates that there is no pressure drop along the length of the pipe and the pressure drop across all the fractures is the same. Applying this criteria to Equation 4.4 gives Equation 4.12. When Equation 4.12 is equated to Equation 4.3, it gives $'q_1 = q_2'$, meaning all of the fracture will take an equal amount of fluid.

$$P_{out}^2 = P_{in}^2 - f_{F\,q1}\frac{2x_L}{d_h}\rho\left(\frac{q_1}{A_f}\right)^2 \qquad (4.12)$$

The second method is to assume that the diameter of the pipe is very large. This indicates that the fluid is free to flow inside the pipe with negligible frictional losses. This would again diminish the pressure loss term due to friction in the equation, giving us equal flow in all the fractures.

The third method is to see what happens if the fracture spacing is unrealistically small. As the fracture spacing lies in the numerator of the pipe frictional loss term, it diminishes and gives an almost equal flow rate in all the fractures. This shows that the equations are valid for all types of flow scenarios.

4.5.3 Relation of Width with Pressure

Flow through a planar fracture is facilitated by the width of the fracture. The permeability of an unpropped fracture is taken to be derived from lubrication theory. Assuming that the fracture is a highly conductive channel (very high permeability – approaching infinite conductivity), the width of the fracture can be defined as the function of injection pressure. For vertical fractures, when the pressure inside the fracture exceeds the minimum total horizontal stress exerted by the formation, it creates a channel to

facilitate the flow. Many studies have been carried out to study the correlation between fracture width and the injection pressure.

One relation between the fracture width and the pressure is given by Witherspoon et al. [10]. It is a cubic law given for a laminar flow between two parallel plates. Equation 4.13 represents this well-known cubic relationship, with Q as the total flow rate, Δh as the difference in hydraulic head, b as the half width between the two plates, and C as a constant that depends on the geometry of the fracture. For a radial flow with well radius of r_w and a fracture radius of r_e, C is given in Equation 4.14. For a straight line flow in a rectangular fracture of length L and width W, C is given in Equation 4.15.

$$\frac{Q}{\Delta h} = C(2b)^3 \tag{4.13}$$

$$C = \left(\frac{2\pi}{ln\left(\frac{r_e}{r_w}\right)}\right)\left(\frac{\rho g}{12\mu}\right) \tag{4.14}$$

$$C = \left(\frac{W}{L}\right)\left(\frac{\rho g}{12\mu}\right) \tag{4.15}$$

Combining Equation 4.13 and 4.15 for a planar fracture gives Equation 4.16. This equation gives a relation between the pressure, flow rate, and width of the fracture, but it does not implement properties of the formation, such as Young's modulus or Poisson's ratio.

$$\left(\frac{12QL\mu}{\Delta P}\right)^{\frac{1}{4}} = w \tag{4.16}$$

Another relation was given by Sneddon and Elliott [11] by studying the opening of a Griffith crack under internal pressure. This equation was further modified by Perkins and Kern [12], giving a fracture width equation. This gives a relation between the injection

pressure and the width of the fracture and also accounts for the formation properties. According to Sneddon and Elliott, for a three-dimensional, radially symmetrical fracture with radius$'C'$, the width of the fracture at any radius is approximately given by Equation 4.17. This equation was derived by performing a volumetric balance of injected fluid into the fracture. The fracture is concave in nature and therefore its width varies with radius, with the maximum width being at the center; that is at $r = 0$ (see Equation 4.18). The average width for the entire fracture can be calculated by taking the volumetric average. The average width of the fracture is shown in Equation 4.19. In all three equations, the pressure (P_{avg}) used to calculate the average width is the average of the injection and the outlet pressure for that particular fracture. $'E'$ Represents Young's modulus of the rock, 'ν' represents the Poisson's ratio for the rock, and $'\sigma'$ represents the total perpendicular stress acting on the fracture surface due to the formation rock.

$$w_r = \frac{8(P_r - \sigma)C(1-\nu^2)}{\pi E}\sqrt{1-\left(\frac{r}{C}\right)^2} \qquad (4.17)$$

$$w_{max} = \frac{8\left(P_{avg} - \sigma\right)C(1-\nu^2)}{\pi E} \qquad (4.18)$$

$$w_{avg} = \frac{2}{3}w_{max} = \frac{16\left(P_{avg} - \sigma\right)C(1-\nu^2)}{3\pi E} \qquad (4.19)$$

As the fluid passes through the fracture, it loses pressure due to frictional loss. Consequently, the fracture should have the maximum width at the injection point (as the pressure is maximum) and the minimum width at the outlet point (as the pressure is minimum) in a fracture. This forms a trapezoidal shape for the fracture. By taking the area average of the inlet and outlet pressure for a given fracture, Equation 4.20 gives the average pressure in the fracture, which gives the planar circular fracture with uniform width.

$$P_{avg} = \frac{(2P_{in} + P_{out})}{3} \qquad (4.20)$$

4.6 Results and Discussion

We have considered a system of wells with a well spacing of 200m, and consisting of 10 fractures, with a fracture spacing of 50m. The flow rate in the system was maintained at $500\ m^3/day$, with an injection pressure of $33500\ kPa$. The other properties of the system and properties of the formation are summarized in Table 4.1.

The flow inside the fracture is assumed to be laminar and the Fanning friction factor for laminar flow is given by Equation 4.21, where Re_f is the Reynolds' number

$$f_{F\,qn} = \frac{16}{Re_f} \qquad (4.21)$$

The flow inside the pipe is also assumed to be laminar and the Fanning friction factor for laminar flow inside the cylindrical pipe is approximated by Haaland's equation, Equation 4.22.

$$\frac{1}{\sqrt{f_{P\,qn}}} = -1.8\ \log\left[\left(\frac{\varepsilon/_D}{3.7}\right)^{1.11} + \frac{6.9}{Re_p}\right] \qquad (4.22)$$

Using the foregoing equations and performing 500 iterations gives the result of flow distribution for a system with ten fractures (Table 4.2). It is evident that the 10th fracture (at the heel) takes the largest amount of fluid.

4.6.1 Effects of Flow Rates in Fixed Number of Fractures

An evaluation was conducted to study the effect of variable flow rates ranging from $100\ m^3/day$ to $2000\ m^3/day$, in a system consisting of ten fractures with a constant

pressure of $34500\ kPa$. The results are plotted in Figure 4.7.

Again, the last fracture (10^{th} fracture) takes the most fluid of all of the fractures, whereas the 1^{st} fracture (at the toes of the wells) takes the least amount in all the cases. Also, when the flow rate is high ($2000\ m^3/day$), the distribution is much skewed towards the last fracture (at the heel) and reduction in the preferential flow into this last fracture is observed with reduction of the flow rate. It is also observed that the last fracture has the maximum width whereas the first fracture has the minimum width.

This can be explained because when the flow rate is low, the frictional losses in the injection and production tubulars are low as well. This means that there is a low pressure drop between two consecutive fractures and hence gives a fairly even distribution amongst the fractures. Alternatively, when the flow rate is high, the frictional losses are high and this creates high resistance to flow in the tubulars, and only a small amount of water circulates into the other fractures. Hence all of the fluid tries to enter into the first fracture it encounters while being injected (that is the last fracture in the system with numbering beginning from the toe of the well). Another reason the fluid tries to enter into the fracture nearest to the heel is because it has maximum width. The width of the fracture is a function of pressure inside the fracture, hence, the first fracture at the heel, where the injection pressure is maximum, has the maximum width.

4.6.2 Effects of Number of Fractures with Fixed Flow Rate

In this scenario, all of the parameters except the number of fractures were kept the same as those shown in Table 4.1. The fluid was injected at a rate of $500\ m^3/day$ and at an injection pressure of 33500 kPa. The number of fractures was varied, from ten to two.

As the number of fractures was decreased, the distance between them was increased proportionally, to keep the length of the tubulars equal in the system. The percentage flow distribution among all of the fractures present is plotted in Figure 4.8.

In all cases, the first fracture took the least amount of fluid and the last fracture (in the respective system) took the most fluid. As the number of fractures increases in the system, the distribution skews towards the last fracture. The system with two fractures had the best distribution with the first fracture taking 70% of fluid and the 2nd fracture (last in this system) taking the remaining fluid. In the system with ten fractures, the first fracture took 4% of the fluid and the 10th fracture took the maximum fluid, amounting to 36% of the total fluid.

As the number of fractures was decreased from ten to two, the overall resistance to flow was reduced. However, since the resistance in the pipe is a function of the flow rate, a preference towards the last fracture is still observed (since it has the least resistance with the maximum width).

4.6.3 Effects of Well Diameter with Fixed Number of Fractures and Flow Rate

To study the effect of pipe diameter on the flow distribution in a doublet system, all of the parameters were kept the same as in Table 4.1, except that the diameter of the injection and production well were varied. The diameter of each tubular section was varied from 6 inches to 10 inches, and the flow distribution amongst the 10 fractures was plotted in Figure 4.9.

It was observed that the pipe with least diameter has a distribution that is largely skewed towards the last fracture (10th fracture) and the pipe with the maximum diameter

had fairly even distribution among the fractures.

The difference in the flow distribution with diameter of the pipe is observed because of the resistance in the pipes. A small diameter would restrict the fluid flow and create significant frictional resistance between consecutive fractures, reducing the tendency to acquire more fluid. However, when the diameter of the pipe is fairly large, the resistance inside the pipe is minimized and the distribution of fluid is even among all of the fractures.

4.7 Conclusions

It is important to plan for and design fracture spacing to control the flow distribution in an EGS, to ensure that the fluid is evenly distributed in all of the fractures so that the heat is being extracted from the complete reservoir.

Equations 4.9 and 4.10 are the basic relationships. These are flexible enough to be applied to any doublet system and study the flow distribution in it. Since the resistance to flow is a function of the volumetric flow rate, the system of equations needs to be iterated until a converged solution is obtained. The other parameters required to solve these equations include a relation between the injection pressure and width of the fracture, a relationship to calculate the frictional loss in the tubulars, a relationship for calculating the frictional loss in the fracture, and a reasonable initial fluid distribution in the fractures (can be calculated by considering a polynomial distribution).

There are many factors that affect the fluid distribution among the fracture. The most important are the injection pressure and the injection flow rate. Optimization of the flow (even distribution) is possible and can be achieved by manipulating the controllable engineering parameters.

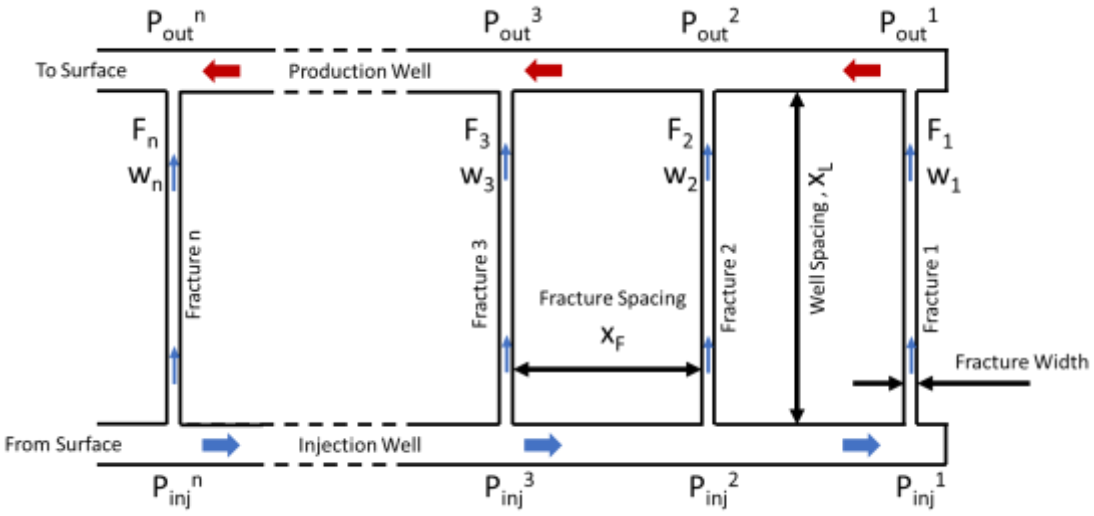

Figure 4.1: Schematic diagram of a rudimentary EGS – one injector, one producer, and n interconnecting infinite conductivity hydraulic fractures.

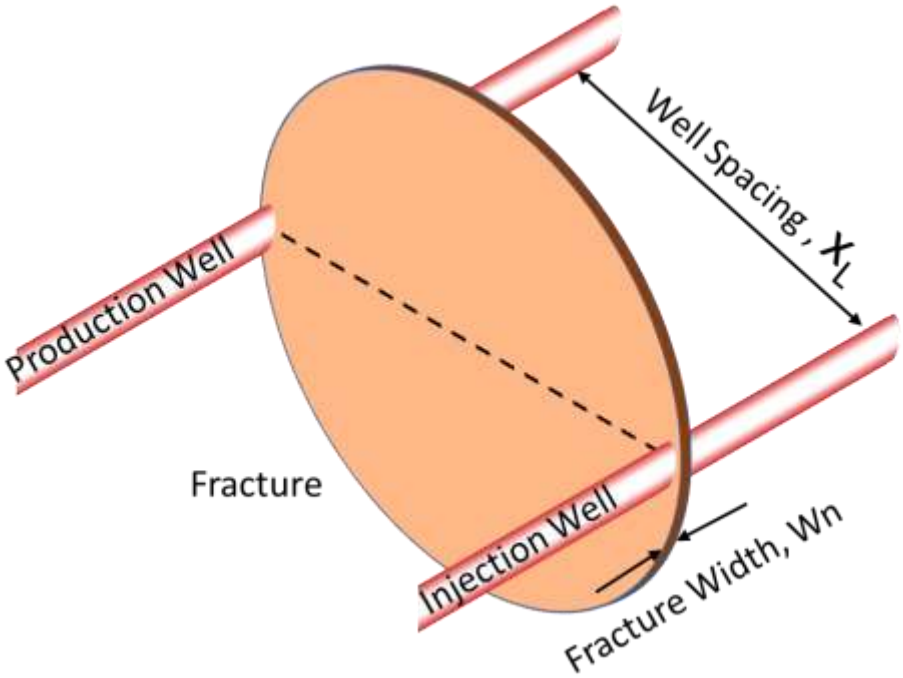

Figure 4.2: Representation of a planar penny shaped fracture (one of many) for the doublet system.

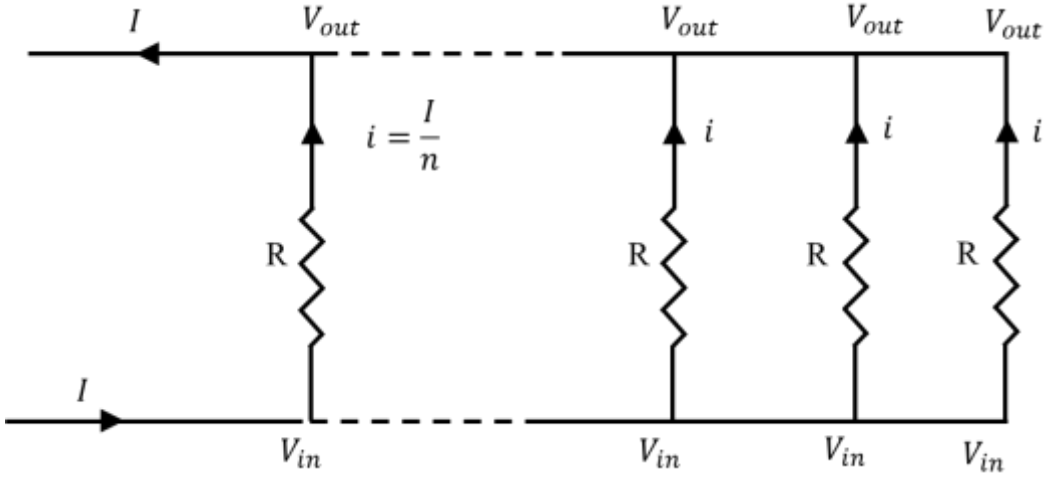

Figure 4.3: Current distribution in a circuit with '***n***' branches of equal resistance.

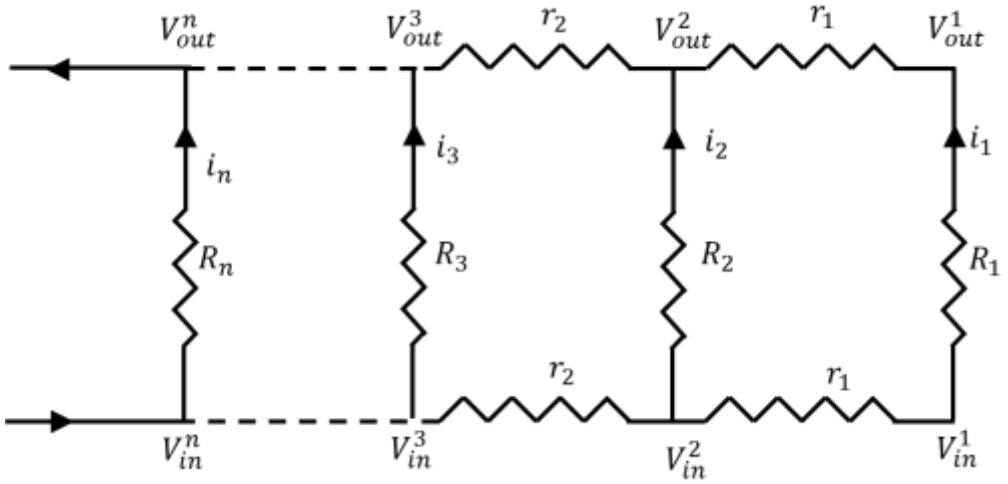

Figure 4.4: Current distribution in a circuit with multiple resistance.

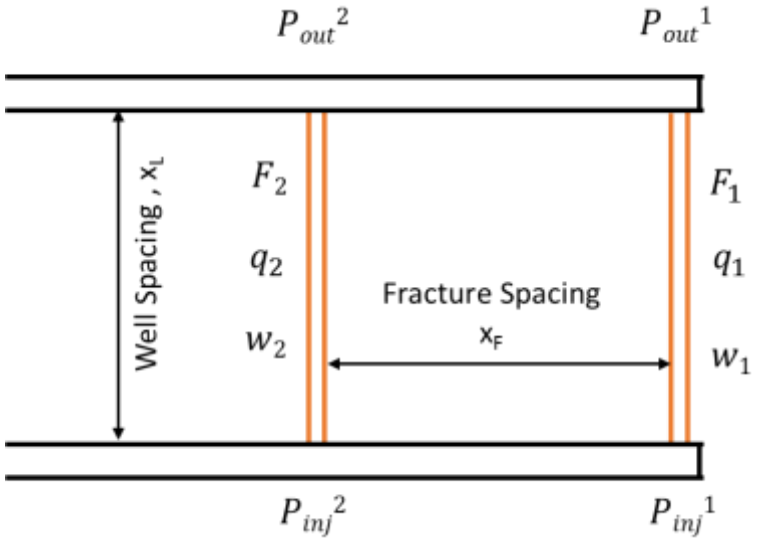

Figure 4.5: Flow distribution in a two fracture system.

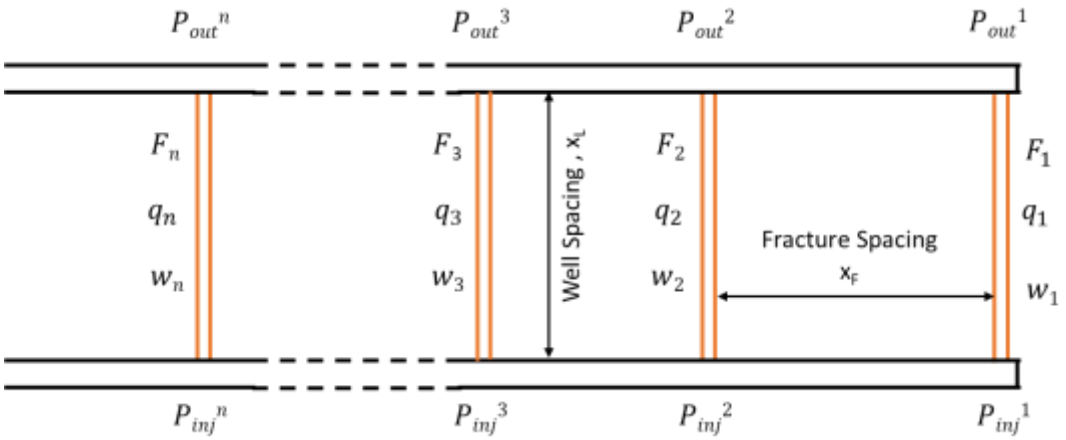

Figure 4.6: Flow distribution in a multifracture system consisting of n fractures.

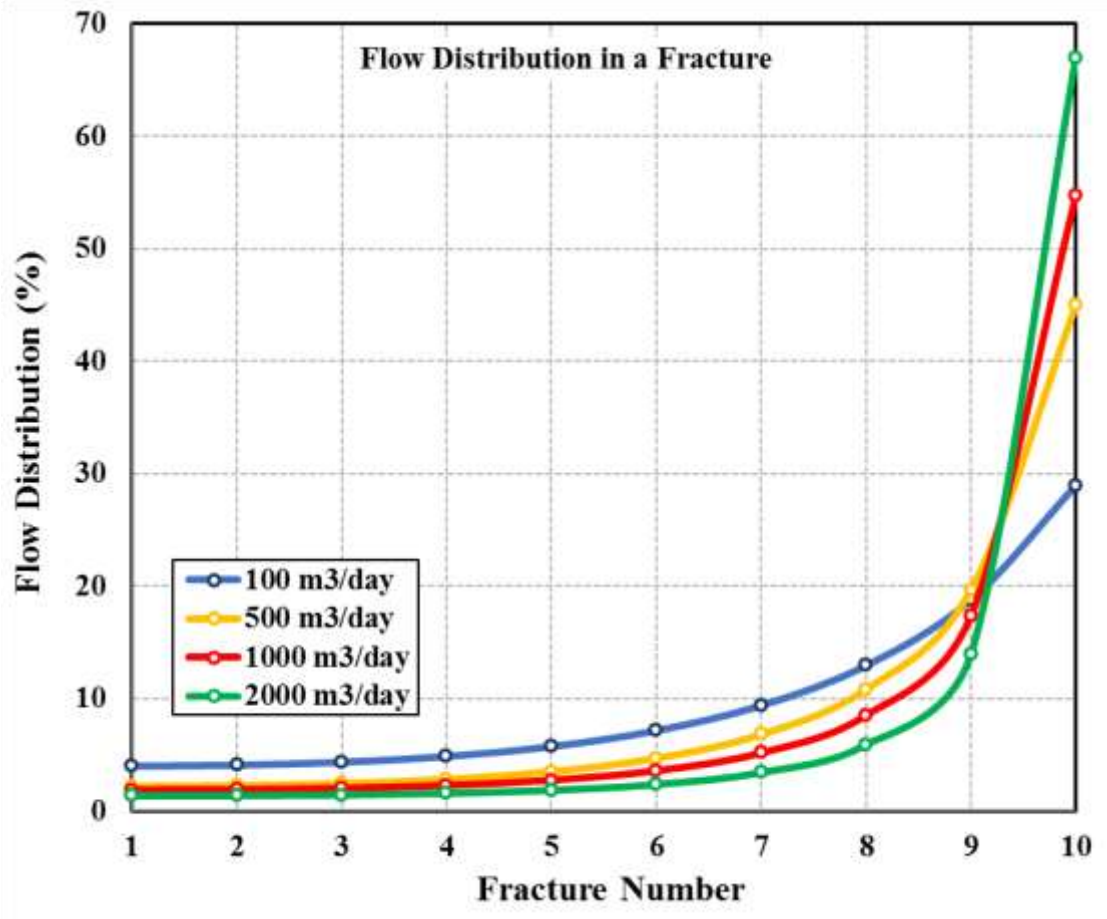

Figure 4.7: Flow distribution among fractures when water is injected at different flow rates.

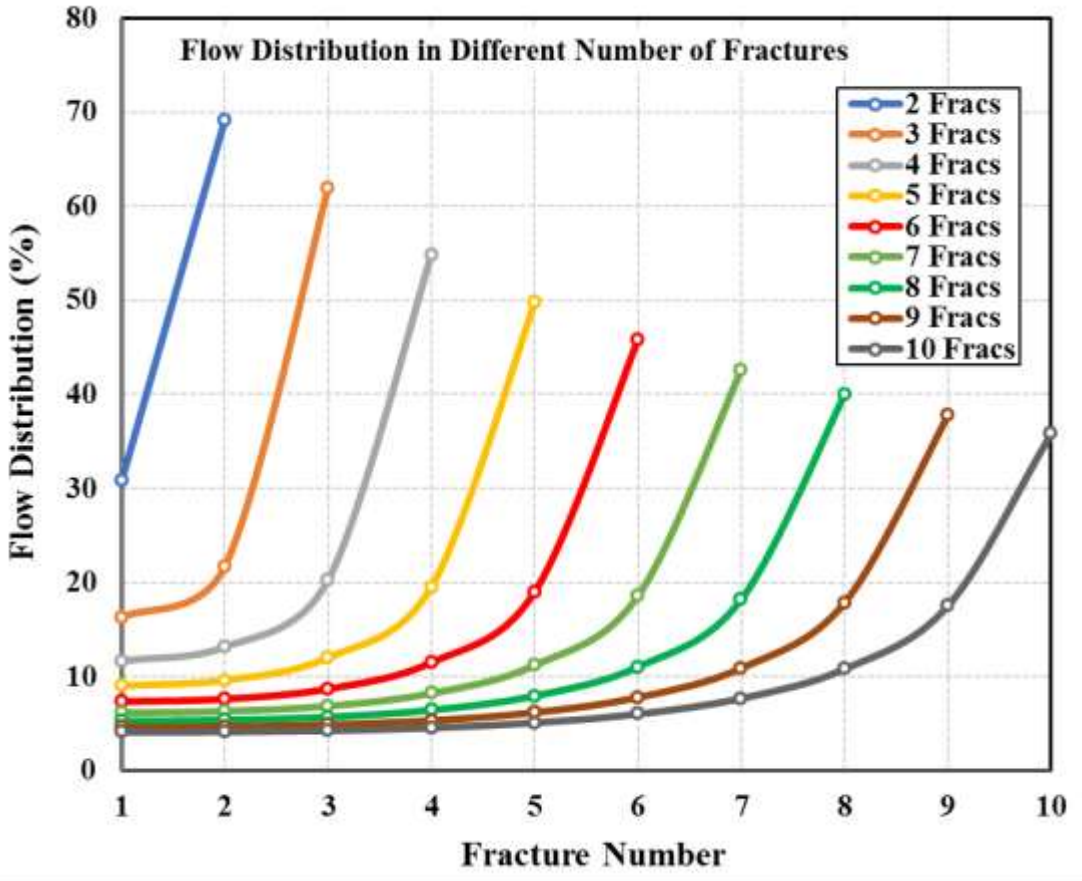

Figure 4.8: Flow distribution among fractures when the water is injected at different flow rates.

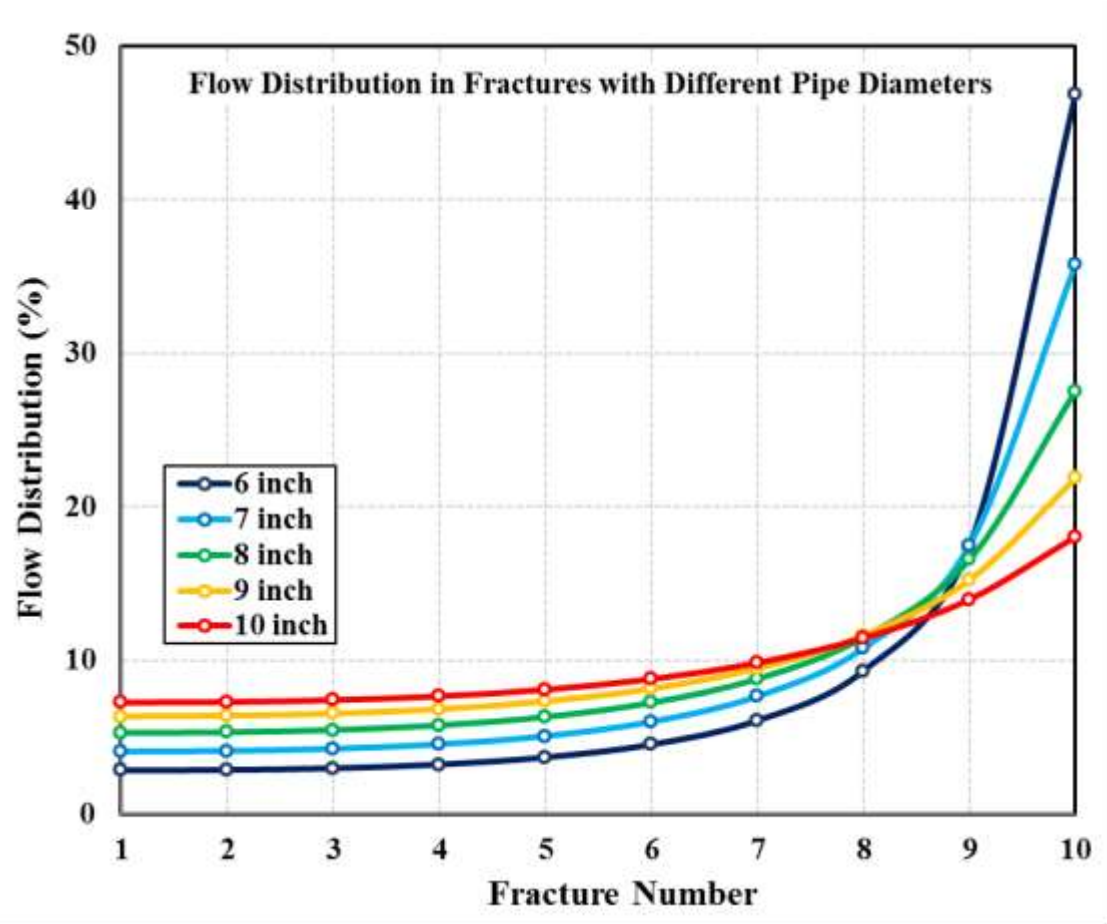

Figure 4.9: Flow distribution among fractures when the well bore diameter is changed.

Table 4.1: Values doublet EGS system

Parameter	Value
Flow Rate, Q (m3/day)	500
Diameter of Pipe, Dp (m)	0.1778
Roughness of Pipe, e (mm)	0.0015
Injection Pressure (kPa)	33500
Poisson's Ration, ν	0.33
Young's Modulus, E (kPa)	62052815.6
Injection Pressure, P_{in} (kPa)	33500
Horizontal Stress, σ (kPa)	31670
Number of Fractures	10
Fracture Spacing (m)	50
Well Spacing (m)	200
Radius of the circular fracture (m)	100

Table 4.2: Flow distribution for 10 fracture system

Frac No.	Flow Rate (m3/day)	Percentage (%)	Width (m)	P in (kPa)
1	20.445	4.089	0.002739	32795.644
2	20.641	4.128	0.002745	32797.822
3	21.318	4.264	0.002764	32805.544
4	22.775	4.555	0.002803	32821.801
5	25.452	5.090	0.002872	32849.942
6	30.132	6.026	0.002980	32894.413
7	38.418	7.684	0.003144	32961.998
8	54.068	10.814	0.003394	33064.454
9	87.679	17.536	0.003785	33225.159
10	179.072	35.814	0.004454	33500.000
Total	500	100		

4.8 List of Symbols

Symbols	Description
F_n	Fracture number, starting from toe of the well
w_n	Width of the n^{th} fracture, m
X_L	Well spacing, m
X_F	Fracture spacing, m
Q	Total flow rate in the system, m^3/day
q_n	Flow rate in the n^{th} fracture, m^3/day
R_n	Resistance number, starting from last branch of the circuit, Ohm
V_{in}^n	Voltage at inlet of the n^{th} resistance, Volts
V_{out}^n	Voltage at outlet of the n^{th} resistance, Volts
i_n	Current in the n^{th} resistance, Amperes
ρ	Density of fluid, kg/m^3
A_p	Cross sectional area of well, m^2
A_f	Maximum cross sectional area of fracture, m^2
g	Magnitude of gravitational force, m/s^2
μ	Fluid viscosity, Pa.s
σ	Total perpendicular stress acting on the fracture, Pa
E	Young's modulus, Pa
ν	Poisson's ratio
ε	Roughness of the pipe, m

4.9 Appendix

Flow distribution in a three fracture system, as shown in Figure 4.23, can be derived by using the pressure drop equations given by Equation 4.23 (pressure drop across a fracture) and Equation 4.24 (pressure drop across a pipe section between two fractures).

$$\Delta \boldsymbol{P}_{\boldsymbol{frac},\ \boldsymbol{n}} = \boldsymbol{f}_{\boldsymbol{f_{qn}}} \frac{\boldsymbol{2X_l}}{\boldsymbol{d_h}} \boldsymbol{\rho} \left(\frac{\boldsymbol{q_n}}{\boldsymbol{A_f}} \right)^{\boldsymbol{2}} = \boldsymbol{b}_{\boldsymbol{F_{qn}}} (\boldsymbol{q_n})^{\boldsymbol{2}} \qquad (\boldsymbol{4.23})$$

$$\Delta P_{pipe,\ n} = f_{p_{q_n}} \frac{2X_f}{D_h} \rho \left(\frac{q_{p,n}}{A_p} \right)^2 = b_{P_{qn}} \left(q_{p,n} \right)^2 \qquad (4.24)$$

So considering only the last two fractures (1 and 2), the flow distribution can be given according to Equation 4.7 and 4.8. Equation 4.25 and 4.26 represent the flow distribution in the last two fractures in a three fracture system.

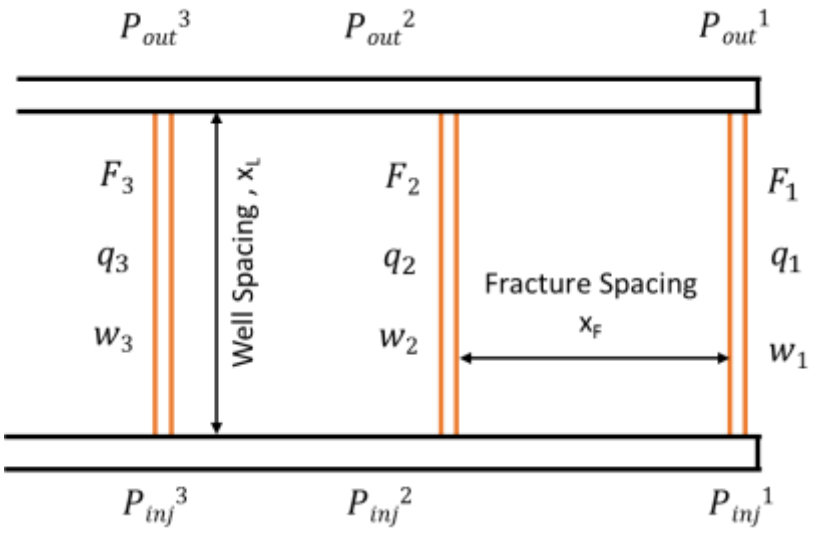

Figure 4.10: Flow distribution in a three fracture system.

$$q_1 = (Q - q_3)\frac{1}{\left(\frac{2b_{P_{q1}} + b_{F_{q1}}}{b_{F_{q2}}}\right)^{\frac{1}{2}} + 1} \qquad (4.25)$$

$$q_2 = (Q - q_3)\frac{\left(\frac{2b_{P_{q1}} + b_{F_{q1}}}{b_{F_{q2}}}\right)^{\frac{1}{2}}}{\left(\frac{2b_{P_{q1}} + b_{F_{q1}}}{b_{F_{q2}}}\right)^{\frac{1}{2}} + 1} \qquad (4.26)$$

The resistance in the Equation 4.26 can be clubbed together to get an equivalent resistance $'c_2'$, as shown in Equation 4.27.

$$c_2 = \frac{\left(\frac{2b_{P_{q1}} + b_{F_{q1}}}{b_{F_{q2}}}\right)^{\frac{1}{2}}}{\left(\frac{2b_{P_{q1}} + b_{F_{q1}}}{b_{F_{q2}}}\right)^{\frac{1}{2}} + 1} \qquad (4.27)$$

The flow in the second fracture is given as Equation 4.28.

$$q_2 = (Q - q_3)c_2 \qquad (4.28)$$

For the third fracture ${P_{out}}^3$, can be calculated directly by subtracting the pressure drop across the third fracture (see Equation 4.29) and also by traversing through the pipe section, the second fracture, and another pipe section (see Equation 4.30).

$${P_{out}}^3 = {P_{in}}^3 - b_{F_{q3}}(q_3)^2 \qquad (4.29)$$

$${P_{out}}^3 = {P_{in}}^3 - 2b_{P_{qn}}(Q - q_3)^2 - b_{F_{q3}}{q_2}^2 \qquad (4.30)$$

Equating Equation 4.29 and 4.30 gives Equation 4.31

$$2b_{P_{q2}}(Q - q_3)^2 + b_{F_{q2}}{q_2}^2 = b_{F_{q3}}{q_3}^2 \qquad (4.31)$$

Substituting Equation 4.28 in Equation 4.31 gives Equation 4.32

$$2b_{P_{q2}}(Q - q_3)^2 + b_{F_{q2}}(Q - q_3)^2(c_2)^2 = b_{F_{q3}}{q_3}^2 \qquad (4.A.32)$$

Equation 4.32 can be solved further to calculate value of q_3. The value of q_3 is given by Equation 4.33.

$$q_3 = Q\frac{\left(\frac{2b_{P_{q2}} + b_{F_{q2}}(c_2)^2}{b_{F_{q3}}}\right)^{\frac{1}{2}}}{\left(\frac{2b_{P_{q2}} + b_{F_{q2}}(c_2)^2}{b_{F_{q3}}}\right)^{\frac{1}{2}} + 1} \qquad (4.33)$$

Equation 4.33 for q_3 is in the same form as Equation 4.26 for q_2. Hence, a generalized equation can be written in the form of equivalent resistance for the n^{th} fracture as shown in Equation 4.34 and the flow through the n^{th} fracture is given by Equation 4.35.

$$c_n = \frac{\left(\frac{2b_{P_{q(n-1)}} + b_{F_{q(n-1)}}\left(c_{(n-1)}\right)^2}{b_{F_{qn}}}\right)^{\frac{1}{2}}}{\left(\frac{2b_{P_{q(n-1)}} + b_{F_{q(n-1)}}\left(c_{(n-1)}\right)^2}{b_{F_{qn}}}\right)^{\frac{1}{2}} + 1} \qquad (4.34)$$

$$q_n = \left(Q - \left(\sum_{i=n}^{N} q_{n+1}\right)\right)c_n \qquad (4.35)$$

For the first fracture, there is no pipe section, hence $b_{P_{q1}} = 0$. This implies that the value of c_1 is '1' to get Equation 4.25 in the general form.

4.10 References

[1] A. S. Batchelor, "The Creation of Hot Dry Rock Systems by Combined Explosive and Hydraulic Fracturing," presented at the Proceedings of the International Conference on Geothermal Energy, May, Florence, Italy 1981.

[2] F. H. Cornet, "Experimental investigations of forced fluid flow through a granite rock mass," presented at the Proceedings of 4th International Seminar on the Results of EC Geothermal Energy Demonstration, April 27-30, Florence, Italy, 1989.

[3] Y.C. Zeng, N.Y. Wu, Z. Su, X.X. Wang, and J. Hu, "Numerical simulation of heat production potential from hot dry rock by water circulating through a novel single vertical fracture at Desert Peak geothermal field," Energy, vol. 63, pp. 268-282, 2013.

[4] B. Guo, P. Fu, Y. Hao, C. A. Peters, and C. R. Carrigan, "Thermal drawdown-induced flow channeling in a single fracture in EGS," Geothermics, vol. 61, pp. 46-62, 2016.

[5] S. Al-Rbeawi, "Analysis of pressure behaviors and flow regimes of naturally and hydraulically fractured unconventional gas reservoirs using multi-linear flow regimes approach," Journal of Natural Gas Science and Engineering, vol. 45, pp. 637-658, 2017.

[6] Y. Zeng, L. Tang, N. Wu, and Y. Cao, "Analysis of influencing factors of production performance of enhanced geothermal system: A case study at Yangbajing geothermal field," Energy, vol. 127, pp. 218-235, 2017.

[7] T. Li, S. Shiozawa, and M. W. McClure, "Thermal breakthrough calculations to optimize design of a multiple-stage Enhanced Geothermal System," Geothermics, vol. 64, pp. 455-465, 2016.

[8] B. Wu, X. Zhang, R. G. Jeffrey, A. P. Bunger, and S. Jia, "A simplified model for heat extraction by circulating fluid through a closed-loop multiple-fracture enhanced geothermal system," Applied Energy, vol. 183, pp. 1664-1681, 2016.

[9] Y. Xia, M. Plummer, E. Mattson, R. Podgorney, and A. Ghassemi, "Design, modeling, and evaluation of a doublet heat extraction model in enhanced geothermal systems," Renewable Energy, vol. 105, pp. 232-247, 2017.

[10] P. A. Witherspoon, J. S. Y. Wang, K. Iwai, and J. E. Gale, "Validity of Cubic Law for Fluid Flow in a Deformable Rock Fracture," Water Resources Research, vol. 16, pp. 1016-1024, 1980.

[11] I. N. Sneddon and H. A. Elliott, "The Opening of a Griffith Crack under Internal

Pressure," Quarterly of Applied Mathematics, vol. 4, pp. 262-267, 1946.

[12] T. K. Perkins and L. R. Kern, "Widths of Hydraulic Fractures," Journal of Petroleum Technology, vol. 13, pp. 937-949, 1961/9/1/ 1961.

CHAPTER 5

CONCLUSION

5.1 Original Contributions

5.1.1 Simulating Small Sections to Evaluate the Performance of Entire Reservoir

Simulating an entire EGS reservoir can be time consuming and quite demanding in terms of computational requirements. By simulating two or three small sections, each containing two fractures, and scaling up the results gives good enough results to evaluate the performance of the entire reservoir for the given set of parameters. This technique is time efficient, requires much less computational capabilities, and can be used for any kind of doublet well configuration, as long as the temperature gradient in the reservoir is constant.

5.1.2 Categorizing EGS Parameters on Basis of their Implementation Stages

To establish EGS, the primary requirement is to have a good geothermal reservoir. The properties of any EGS can be grouped into three categories, namely natural properties (in-situ), completion parameters, and operational parameters. The first stage for development of EGS is to evaluate the natural properties of geothermal reservoirs (like reservoir temperature, heat capacity, thermal conductivity, etc.) and choose a desirable location. The natural properties give us the total heat content of the reservoir. The next

stage is completion, and the completion parameters (like well spacing, fracture spacing, number of wells, etc.) would determine the recovery factor for the given reservoir, depending on the area it is able to cover. The last stage is the operations and the operational parameters (like flow rate, injection temperature, type of fluid, etc.) would determine the rate of heat extraction and hence determine the life of the system.

5.1.3 Optimizing the Heat Extraction, by Ranking the Parameters

It is important to understand the effect of each parameter on the total amount of heat extraction in a given period of time, and also to what extent it affects it. One way to do this to carry out multiple simulations by varying one parameter at a time, while keeping all other parameters as constants. This would give a range in terms of performance for a varied parameter. The information can be then used to evaluate which parameter has the maximum effect and which has the least effect. The EGS can be then designed accordingly to get optimal performance.

5.1.4 Developing Flow Distribution Equation for Multifractured Doublet System

In an EGS having multiple fractures along its lateral, it is important to know how the fluid is getting distributed among the fractures to optimize the heat extraction. The flow equations were developed using Kirchhoff's law for current distribution as an analogy. The frictional losses in the pipe and inside the fractures were considered as resistance and the flow rate was considered analogous to the current with pressure drop acting similar to the potential drop. Using this, a generalized flow equation was derived. As the frictional losses are a function of the flow rate (velocity), the equations developed were implicit in nature

and hence required to be iterated until convergence to get the flow distribution.

5.2 Future Scope of Study

EGS is a relatively younger field of study and still has much untapped potential. Currently the efficiencies for a closed loop EGS using ORC (Organic Rankine Cycle) are around 10-15%, which is quite low. As the efficiency of the system is a function of the temperature of produced water, it is important to optimize the system to achieve higher temperatures. A study focused on evaluation and development of multilateral EGS would help in overcoming the efficiency barrier. Different well configurations like triplet (one injection and two production wells), star (one injection well in the center surrounded by four production wells), and others need to be studied to evaluate their performance.

Another important field of study includes development of better hydraulic fractures at optimized spacing to have the maximum surface area for heat extraction. Also, the fluid distribution in multifractured EGS needs to be optimized to make sure heat is evenly withdrawn from the system.